ESRF NEWSLETTER

SEPTEMBER 1998 EUROPEAN SYNCHROTRON RADIATION FACILITY N° 31

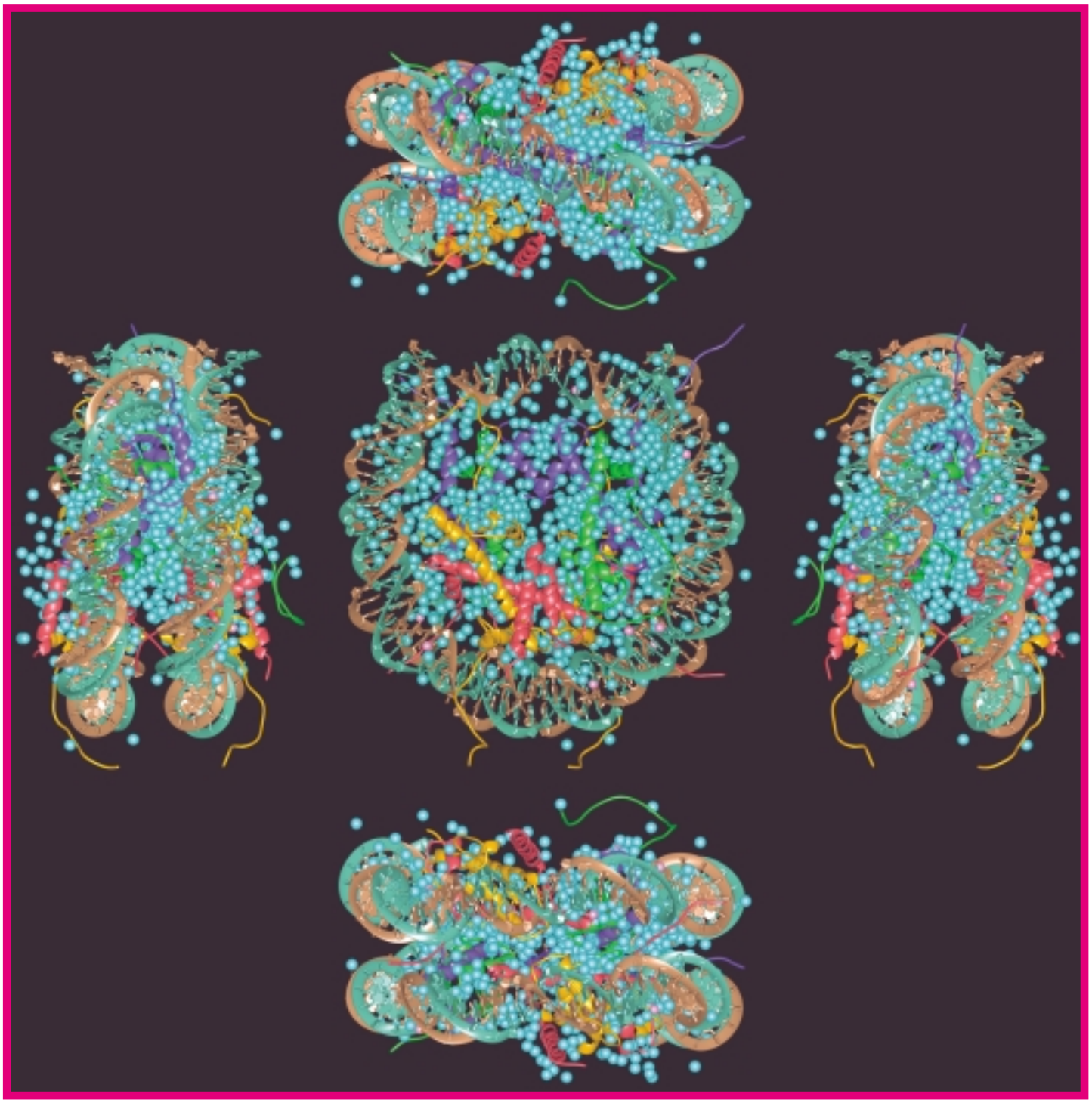

Multiple views of the nucleosome core particle crystal structure at 2.0 Å resolution. Over 800 water molecules (cyan) and divalent ions (magenta) have been added to the more than 12,000 C,N,O atoms of the proteins and DNA that make up this fundamental repeating unit found in chromosomes (see article on page 9).

ISSN 1011-9310

CONTENTS

Photography by:
C. Argoud,
B. Denis (Art Photos).

PRIZE GIVEN FOR SR COMPUTED TOMOGRAPHY PERFORMED ON ANIMALS

At the 6th Conference "Biophysics & Synchrotron Radiation", from 4 to 8 August 1998 at Argonne in the USA, a prize was given for the poster presented by G. Le Duc, A.-M. Charvet, H. Elleaume and F. Esteve, from the Jeune Equipe RSRM (Univ. Joseph Fourier in Grenoble) and the ESRF Medical Beamline. This Jeune Equipe were the first to perform brain tomography on an anesthetized animal (a rat).

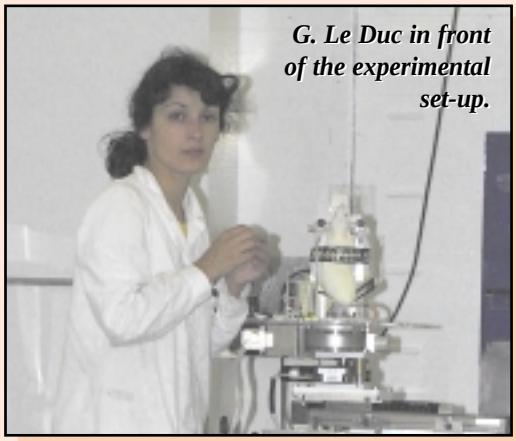

G. Le Duc in front of the experimental set-up.

29th Council Meeting

At its 29th meeting on 9 and 10 June 1998 in Grenoble, the ESRF Council took several decisions which will have an impact on the medium-term future of the institute.

Israel as new Scientific Associate

The Council agreed to, and authorized its Chairman to sign for the ESRF on its behalf, an «Arrangement between the Government of the State of Israel and the European Synchrotron Radiation Facility concerning the long-term scientific use of synchrotron radiation for non-proprietary research» very similar to the one concluded last year with Portugal (cf. ESRF Newsletter n° 29, p. 3).

Since the Foundation Phase of the ESRF, contacts have been made with the Israel Academy of Sciences and Humanities concerning an involvement of Israel in the ESRF. In February 1987, the then Israeli Minister of Science and Development, Gideon Patt, considered in a letter to the Chairman of the provisional ESRF Council, Pierre Agrain, an application for Israel to become a full Member of the ESRF. In the outcome, however, Israel was not among the founding Members of the ESRF. Nevertheless, regular visits by Israeli scientists over the last ten years have marked the continuous interest of the Israeli scientific community. However, it was obvious that its size would not match the 4% threshold required for full ESRF Membership.

Discussions with the Israeli partners intensified after the Council had clarified the conditions for long-term arrangements in accordance with Article 8 of the ESRF Convention. The arrangement agreed by the Council is due to be signed in November in Jerusalem and will make Israel the second Scientific Associate of the ESRF. Thus scientists from Israel will have the same rights of access to the ESRF beamlines as those from the twelve Contracting Party countries. For the time being, the level of the Israeli contribution to the ESRF operating costs has been set at 1% of the contributions of the Members.

Membership below 4%?

During the discussion with potential Scientific Associates, the question was raised whether a reduction of the threshold for full Membership to less than 4% could be considered in the long term. Following an exchange of views on this issue, the Council noted that almost all delegations wished to maintain the 4% threshold for Membership as provided for by the ESRF Convention and Statutes, and to encourage the participation at lower rates in the form of consortia.

Re-adjustment of contribution rates

The ESRF Convention determines the contribution rates of the different Contracting Parties. In the event of a lasting and significant imbalance between scientific use and contributions, it also provides for the option of a re-adjustment of these contribution rates.

With a view to the end of the ESRF construction period and some experience on the use made of the facility since 1994, the Council adopted «Guidelines for the readjustment of contribution rates» which in particular

- clarify the quantitative assessment of the scientific use (taking into account the activity of Collaborating Research Groups and of the GRAAL experiment using γ-rays produced by Compton back-scattering of laser light),
- give a precise meaning to the terms «lasting» and «significant» used in the Convention and
- indicate the procedure to be followed for the implementation of a re-adjustment.

Beam time allocation for macromolecular crystallography

In his report to the Council, the Director General mentioned the strongly increasing numbers of proposals for macromolecular crystallographic studies (some 240 for the second half of 1998) which put a heavy burden on the review committee for life sciences. With the extension of the experimental possibilities at the Quadriga beamline (ID14A+B) a further increase can be expected. Since relatively few groups account for a considerable proportion of the projects that are awarded beam time, Management suggested testing another system: a number of groups within Europe will be identified to whom blocks of beam time will be awarded without prior evaluation of the individual experiment proposals. The *a posteriori* assessed performance record per group will then be essential for whether in the future the block allocation of the group will be continued, changed or removed completely.

The Council noted that such a system (together with several accompanying measures) will be implemented on a trial basis for the next proposal round (concerning the first half of 1999).

Building construction

There is a lack of laboratories and offices at the ESRF due to:

- the increase of personnel (staff, externally funded collaborators, visitors),
- the closure of buildings provisionally acquired for the construction period and,
- the increasing needs of Collaborating Research Groups, etc.

There is still some potential to further extend the Experimental Hall, both at the outer and inner circumferences, or to add further satellite buildings around the Hall.

The Council took note of the planned construction, starting this year, of further laboratories and offices to satisfy the most urgent needs.

Budget for 1999

The decision on the budgets is usually taken at the autumn meeting of the Council. With a view to the tight national budget situation in some of the Contracting Parties countries, the Council so far adopted a ceiling figure of 400 million French Francs for new contributions from Members to the budget of 1999 (which is 1.0% more than the amount of Members' contributions to the current budget of 1998).

Reduction of working time

The Council

- noted that the French legislation on working time will change but that the corresponding application texts were not yet available, and

… 29th Council Meeting

• asked Management to prepare, as soon as possible, information about both the regulatory and the financial consequences of these changes for the ESRF.

This item was also raised by the representatives of the ESRF in their meeting with the Council.

Director of Administration

Prior to its meeting, the Council decided by written procedure to extend the appointment of the present Director of Administration, Dr. W.E.A. Davies, up to 31 January 2002.

Guidelines for selecting and appointing ESRF Directors

The Council had a second reading of new guidelines for selecting and appointing ESRF Directors. Much consideration was given to this document due to the fact that during the period of 15 months between January 2001 and March 2002 the contracts of all five ESRF Directors will end and the selection and appointment procedures should begin well beforehand. The Council decided to resume the discussion at its next meeting based on a new draft incorporating the amendments proposed.

Science Advisory Committee

The membership of the present Science Advisory Committee will come to an end on 31 December 1998. Due to the appointment procedure (eleven scientists directly nominated by the Members of the ESRF, a further ten appointed by the Council) the renewal of membership has to be prepared in several phases.

The Council took note of the schedule which shall lead to the appointment of a new Science Advisory Committee at the next meeting of the Council.

K. Witte

HERCULES 1998

The seventh session of the HERCULES course (Higher European Research Course for Users of Large Experimental Systems) took place at the Maison des Magistères, CNRS Grenoble, from 22 February to 3 April 1998. The 79 participants (mostly European or registered in European Universities) were divided in two sessions :

• session A: Neutron and synchrotron radiation for physics and chemistry of condensed matter with 44 full-time participants and 11 part-time participants.

• session B: Neutron and synchrotron radiation for biomolecular structure and dynamics with 24 full-time participants. A special effort has been made towards the community of biologists by opening the course to non-European countries (USA, Brazil...)

The course included lectures, practicals and tutorials as in previous years. As last year, session A was particularly centered on recent developments of neutron and X-ray spectroscopy. New lectures devoted to structural molecular biology have been included in the program of session B: «Medical imaging with synchrotron radiation», «X-ray microscopy», «Nuclear spin contrast variation studies». The publication of the volume IV of the HERCULES series entitled «Structure and dynamics of biomolecules» by Oxford University Press is now in progress. For both sessions, a specific seminar on industrial applications was introduced and appreciated by the participants.

In Grenoble most of the practicals were performed on ESRF beamlines (including the French, Italian and Swiss-Norwegian CRG beamlines) and at the ILL. The collaboration of EMBL, IBS as well as CNRS and CEA-Grenoble was also greatly appreciated. Participants from the two sessions carried out practicals at LURE (Orsay) and the Laboratoire Léon Brillouin (Saclay).

The poster session at the Maison des Magistères (55 posters displayed) was one of the highlights of the course and allowed fruitful exchanges between participants and Grenoble scientists.

HERCULES 99 will follow next year with the same two parallel sessions from 21 February to 1 April 1999.

HERCULES 1999
Higher European Research Course for Users of Large Experimental Systems

Grenoble, 21 February - 1 April 1999

Session A:
«Neutron and synchrotron radiation for physics and chemistry of condensed matter»

Session B:
«Neutron and synchrotron radiation for biomolecular structure and dynamics»

Information:
Secrétariat HERCULES
CNRS - Maison des Magistères
BP 166
38042 Grenoble Cedex 9
Tel: +33 (0) 4 76 88 79 86
Fax: +33 (0) 4 76 88 79 81
e-mail: simpson@polycnrs-gre.fr
http://www.polycnrs-gre.fr/hercules

Deadline for application: 16 October 1998

LIFE SCIENCES LEAD NEW REQUESTS FOR BEAM TIME

Users requesting beam time between August 1998 and January 1999 sent in a record number of 799 new proposals for the 1 March application deadline. This was a 37% increase over the previous period, due mainly to the very large increase in Life Sciences applications, up 242 from 128, an increase of almost 90%. Requests from this community of users reflect a recognition of the exciting results which are increasingly being achieved with the use of synchrotron radiation (see in this Newsletter the article on the nucleosome, on page 9), and the progressive opening of the Quadriga beamline, ID14, with its four independent experimental stations. This beamline is one of the 28 ESRF and 7 CRG beamlines which are expected to be scheduling user experiments during the next period.

Following the meetings of the Review Committees at ESRF on 27 and 28 April 1998, 359 proposals were selected and allocated beam time totalling 4341 shifts. Of these, seven new long term programs were accepted for a period of two years. Details of the requests and allocations, per committee, are summarized in **Table 1**.

Numbers of shifts of beam time requested and allocated per scheduling period since the beginning of user operation in September 1994 are shown in **Figure 1**. It should be noted that the second scheduling period each year to date has been slightly shorter than the first, so that in general fewer shifts have been allocated and scheduled during the second half of each year.

R. Mason

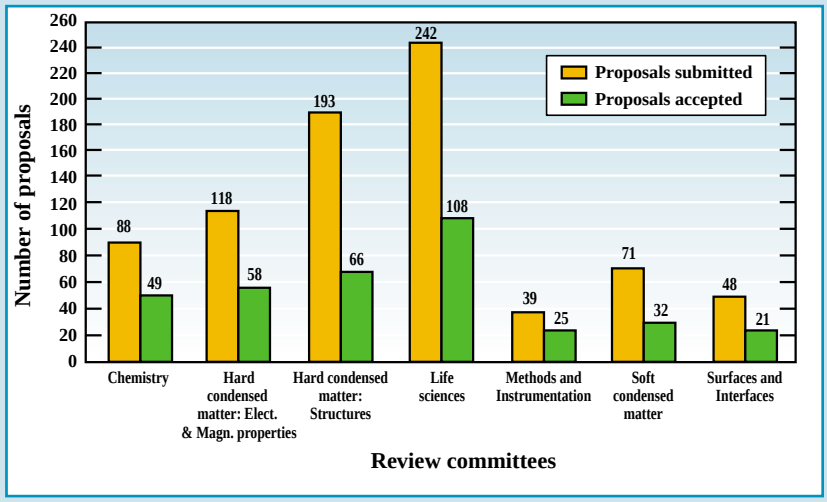

Table 1: Number of proposals per review committee.

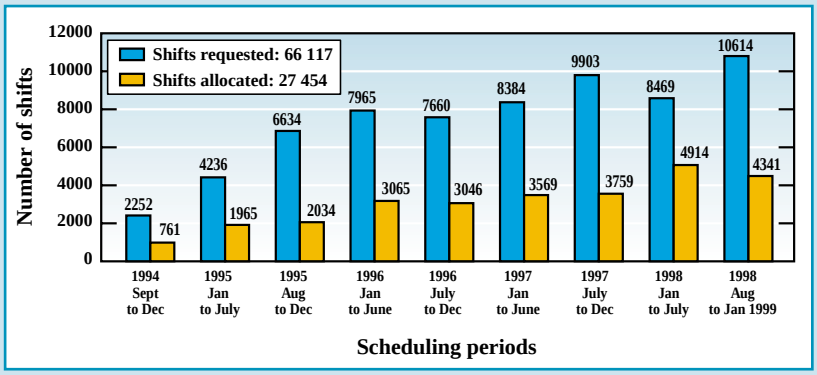

Fig. 1: Total number of shifts of beam time requested and allocated, per scheduling period, 1994 to 1998/II.

USERS' MEETING

11-12 February 1999

The next Users' Meeting will start on Thursday 11 February 1999, with the usual «plenary format», plus posters, plus exhibitors at the Atria conference centre. The change of date from pre- to post-Christmas is for at least two good reasons. Firstly it is in response to requests from users to meet ESRF staff in the «run up» to a submission date in order to benefit from their informal views of project proposals. Secondly it avoids a period when the User Office staff, who help tremendously with the administration of these meetings, are very busy processing the recommendations of the Review Committees. For many users there is also the matter of a few hours on the slopes which was precluded in the pre-Christmas slot!

The meeting will continue with workshops on the Friday, and possibly Saturday, based on the ESRF site, plus adjacent venues if we have more than three viable suggestions. All beamline scientists have been emailed to ask for their suggestions, and just a few have responded. M. Cooper and other members of the Users' Committee need to know NOW if you want to run a workshop. Please contact csmc@spec.warwick.ac.uk or ring M. Cooper in the UK (+44 1203 523379) to discuss the options and put the dates in your diary!

Workshop for Industry «Chemistry and Surfaces»

held on 4 June 1998

The ESRF welcomed about twenty industrialists on 4 June 1998 for the workshop dedicated to chemistry and surfaces.

Participants came from different fields of activities such as chemicals, pulps, metallurgy, cosmetics, polymers, cements, detergents and electronics (l'Oréal, Philips Analytical, Sagem, Rhône Poulenc, Lafarge, Ocas NV, Dow Corning, Rhodia, Arjo Wiggins, BASF, Unilever, Italcementi).

After an introduction by the Director General Y. Petroff, A. Fitch gave a talk entitled «Identification and characterization of crystalline powders by x-ray diffraction». The different uses of powder diffraction were presented as the advantages of synchrotron radiation for this technique. Some examples were given: characterization of ancient Egyptian cosmetics, research on Li-ion plastic electrolyte battery, the structure determination from powders (ex: fluorescein diacetate). This technique is of special interest for industrialists working in polymers and metallurgy.

S. Pascarelli spoke about the perspectives for industrial research using x-ray absorption fine structure spectroscopy at the ESRF. She described the various EXAFS techniques dedicated to bulk materials (transmission), diluted systems (fluorescence), surfaces (reflection), and real-time analysis (dispersive EXAFS). She gave research examples of industrial applications: Er-doped Si for opto-electronics, rare earth-doped glasses for optical fibers, structure of reaction intermediates in solution (alkene oligomerisation), monitoring of chemical oscillations during CO oxidation on Pt supported catalysts. She underlined that the ESRF is much more efficient than the second generation synchrotron sources for the study of ultra-dilute systems (down to a few ppm) and for the study of fast processes (down to the ms resolution).

S. Ferrer gave an overview of surface, interface and thin layer characterization using synchrotron radiation. Three techniques were presented: surface x-ray diffraction, circular magnetic dichroism and total reflection fluorescence analysis. They were illustrated by the microscopy of magnetic domains in ultra-thin films, surface atomic structure of KPD crystals (KH2 PO4) in aqueous solution, and trace element analysis on Si wafers for which a beamline dedicated to industry is under construction at the ESRF (see this Newsletter, page 28).

J. Baruchel presented x-ray imaging at the micrometer scale and its place at the ESRF. Different techniques were described with their applications: microtomography with images of human vertebra samples and PVC foam sample, phase contrast imaging of a polymer sphere with two layers and of a AlSiC composite material, as well as the chemical mapping of fly-ash particles by fluorescence analysis. Several chemical companies already benefit from these new imaging techniques at the ESRF.

Finally, J. Doucet, ESRF Co-ordinator for Industry, explained the reasons for industrial companies to use synchrotron beamlines and presented the different types of collaboration: isolated short characterization, long-term collaboration, pure beam time purchase, full service (data collection + analysis), PhD or post-doc funding, long-term visitors, and even beamline construction and operation.

The afternoon was devoted to the visit of several experimental stations: ID2 (small-angle scattering), ID11 (diffraction), ID13 (microdiffraction and microfluorescence), ID16 (high-resolution powder diffraction) and ID22 (micro-analysis and phase contrast imaging).

J. Doucet

If you are interested, please send us a fax (+33 (0) 4 76 88 24 60) or an e-mail (recruitm@esrf.fr) with your address, and we will provide you with an application form. You can also print out an application form on the World Wide Web http://www.esrf.fr

VACANCIES AT THE ESRF ON 7 AUGUST 1998

	Ref	Subject
POST-DOC	PDID10B-1	Troïka II beamline (ID10B)
	PDBM29/ID26	EXAFS (two positions)
	PDID22	Phase contrast microtomography (ID22)
	EUPD214	Time-resolved protein crystallography
	EUPD215	Proton pumping in membranes
STUDENTS	CFR239	X-ray gyrotropy and related optical phenomena
	CFR243	High resolution residual strain mapping
	CFR244	Soluble, electrically conducting polymers
	CFR245	Micro-structural characterization of cold and hot forming processes
	CFR246	Phase transitions in colloidal systems
ENGINEER	CDD/DP	Software Engineer - 6-month contract
	2209	Mechanical Engineer

Soft Matter under Flow as Probed by Small-Angle Scattering - SASFLOW '98

In the last five years a major challenge among the soft-matter community is to elucidate the relationship between rheological properties of complex fluids and their mesoscopic structure as revealed by small-angle scattering (SAS) experiments. On 28-29 May 1998, a common ESRF/ILL workshop was held at the ESRF, organized by O. Diat (ESRF), P. Lindner and J. Zipfel (ILL).

The main objectives of this common workshop were:

- to advance the new opportunities of experiments under shear on large instruments and especially at the ESRF and ILL.
- to provide a summary of recent experiments or projects using SAS techniques.
- to explore users' interest in order to plan long-term projects and to optimize technical developments and analysis.

This workshop was divided into six sub-sessions, on surfactants, polymer solutions, block-copolymers, polymer blends, suspensions under shear and a session on instrumentation plus a visit to the experimental facilities on the site (ILL and ESRF). A poster session was also organized in order to complement the overview of some recent experiments in this field.

As D. Roux recalled in the first contribution, scattering techniques (light, x-ray and neutron) give the most interesting structural information to understand the phenomenological and mechanical results obtained by rheology. Several examples of shear transitions i.e. transitions to metastable phases or orientation not observable at equilibrium were presented (shear stripping of charged vesicles - Gradzielsky *et al*; «onion phases» - Roux *et al*; shear ordering of surfactant system - Penfold *et al*, Richtering *et al*; shear ordering or shear melting in block-copolymer system either in melt or solution - K. Mortensen *et al*, I. Hamley *et al*, Porte *et al*; shear thickening in polymer-clays mixed system, S. Cocard *et al*). On the other hand, phase transitions under shear or shift of the transition line have also been observed as in vesicle to micelle transition in surfactant mixtures (E. Mendes *et al*), in shear-induced aggregation in polymer solution (I. Morfin *et al*, T. Hashimoto), in shear effects in liquid crystal polymers (L. Noirez *et al*), or in critical polymer mixtures under shear flow (C. Han *et al*), on weakly flocculated dispersions (J. Vermand *et al*) and on diblock copolymer systems with re-entrant phenomenon (H. Leist *et al*). Although we can always present these shear effects as enhancement or decrease of fluctuations along the flow, it is still very difficult to predict them. All these examples are the signature of a large and rich variety of flow behavior completely open to theory [1].

All these groups presented some results using their specific techniques (light or neutron or x-rays). The aim of this common workshop was to find out ways of optimizing the use of the new third generation synchrotron sources (high spatial resolution and time-resolved experiments) as well as high-flux neutron beams (contrast variation) for pertinent experiments. Kinetics studies under continuous or oscillatory shear to describe the out-of-equilibrium transitions have been stressed (Porte *et al*, O. Pelletier *et al*, Mortensen *et al* C. Han *et al*). Moreover, the development of shear cells with an access to the vorticity-gradient plane seems very important due to the effect of phase separation in the Couette cell gap (stress effect instead of shear effect). This also requires the on-line set-up of a rheometer to correlate directly stress measurement and scattering techniques.

The last point but not the least which has been emphasized, is the development of elongational flow systems (spinning system, stagnation point and stretching devices) which are very relevant in areas like materials processing, development of composites as well as in investigations of polymer dynamics in complex geometries (M. Cloitre *et al*).

Some new contacts have already been established and, in common with the ILL, we shall be able to judge the effectiveness of our development only in a few years' time when we look at what will be achieved. A common WEB page will be implemented in order to inform other large instrument beamlines and users about new instrumental development at the ESRF and the ILL.

P. Lindner, J. Zipfel and myself would like to thank all the people who have made this workshop successful.

O. Diat

[1] T. McLeish: Theoretical Challenges in the Dynamics of Complex Fluids, edited by T. McLeish, Kluwer Academic Publishers, Netherlands (1997).

Effect of Shear on Diblock Copolymer Gels

I.W. Hamley[1], J.A. Pople[1], J.P.A. Fairclough[2], A.J. Ryan[2], N.J. Terrill[2], C. Booth[3], G.-E. Yu[3] and O. Diat[4]

1 School of Chemistry, University of Leeds (UK)
2 Department of Chemistry, University of Sheffield (UK)
3 Department of Chemistry, University of Manchester (UK)
4 ESRF, Experiments Division

Low molecular weight block copolymers can behave as amphiphiles in solution, forming lyotropic liquid crystalline phases such as cubic micellar phases. The formation of such structures results in stiff transparent gels which have a number of technological applications for example in drug delivery.

Of particular interest are block copolymers containing hydrophilic poly(oxyethylene) as well as a hydrophobic block such as poly(oxybutylene) or poly(oxypropylene) which are manufactured on a large scale because they behave as surfactants in aqueous solutions. Despite their industrial relevance, surprisingly little is known about phase formation in these systems, nor on the effect of shear on ordered structures which is relevant to processing. Small-angle x-ray scattering (SAXS) has been performed on the ID2 SAXS station to elucidate the effect of shear on the orientation of cubic micellar phases formed by a poly(oxyethylene)-poly(oxybutylene) diblock copolymer in aqueous solution [1,2]. Macroscopic orientation of samples was achieved by shearing in the Couette cell available on ID2 using steady shear. By translation of the Couette cell it was possible to access two orthogonal planes with either the shear direction (**v**) or shear gradient direction (∇**v**) horizontal and the vorticity direction (**e** = ∇**v** x **v**) vertical. Experiments were conducted on the diblock $E_{40}B_{10}$ (here E = oxyethylene, B = oxybutylene and the subscripts denote the number of repeats) in 0.2 M K_2SO_4. A body-centred cubic phase observed for gels with concentrations greater than 30 wt% copolymer was found to orient into a polydomain structure, with the close-packed {110} planes both parallel and perpendicular to the shear plane [1-3]. This is indicated by the SAXS patterns in Figure 1. For gels with 30 wt% copolymer or less, an fcc phase was observed, and this was also observed on heating the more concentrated gels that formed a bcc phase at room temperature [1-3]. The hard gel fcc phase could be oriented to form a highly twinned structure (as shown by the SAXS patterns in Figure 2), with a significant deviation from the ABCABC… stacking sequence of the ideal structure due to random stacking sequences resulting from the slip of {111} hexagonal close-packed planes. For the lower concentration solutions, a transition from hard to soft fcc gels at increasing temperatures was found to be characterized by a change in the susceptibility of the sample to macroscopic shear orientation, as probed using SAXS [2]. The hard gel could be oriented by shear into a twinned fcc structure, whereas the soft gel comprised an fcc phase with a small grain size, which could not be sheared to form a macroscopically oriented domain. Shear only homogenized the sample, producing a powder SAXS pattern [2].

References

[1] J.A. Pople, I.W. Hamley, J.P.A. Fairclough, A.J. Ryan, G.-E. Yu and C. Booth, Macromolecules ***30****, 5721 (1997).*

[2] I.W. Hamley, J.A. Pople, J.P.A. Fairclough, N.J. Terrill, A.J. Ryan, C. Booth, G.-E. Yu, O. Diat, K. Almdal, K. Mortensen and M. Vigild, J. Chem. Phys. ***108****, 6929 (1998).*

[3] I.W. Hamley, J.A. Pople and O. Diat, Colloid Polym. Sci., 276, 446 (1998).

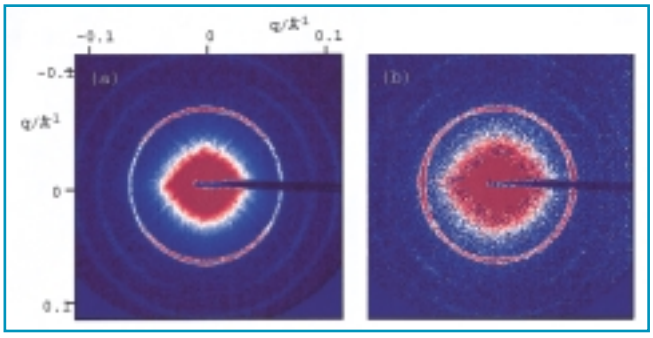

Fig. 1: SAXS patterns for a 38 wt% solution of $E_{40}B_{10}$ in the bcc phase at 25 °C.

(a) (q_v, q_e) plane, during shear at $\dot{\gamma}$ = 8 s^{-1}, (b) q_∇, q_e) plane during shear at $\dot{\gamma}$ = 8 s^{-1}. The vorticity direction is vertical.

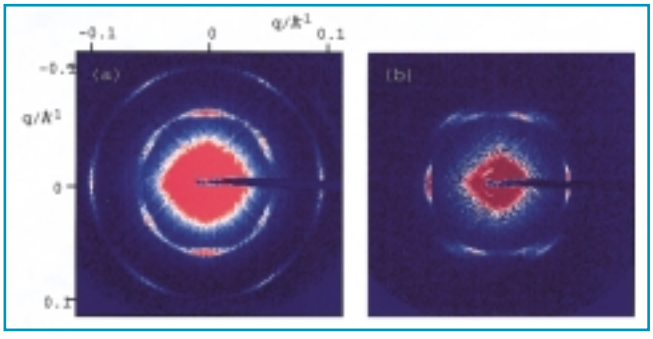

Fig. 2: SAXS patterns for a 38 wt% solution of $E_{40}B_{10}$ in the fcc phase at 52 °C.

(a) (q_v, q_e) plane, during shear at $\dot{\gamma}$ = 0.8 s^{-1}, (b) q_∇, q_e) plane during shear at $\dot{\gamma}$ = 0.8 s^{-1}. The vorticity direction is vertical.

The Atomic Structure of Chromatin's Nucleosome Core Particle at 2 Å Resolution

K. Luger, A. Mäder, D. F. Sargent and T.J. Richmond

Institut für Molekularbiologie und Biophysik, ETH Zürich (Switzerland)

Protein crystallography is currently turning out novel atomic structures of biological macromolecules at the rate of 400-500 per year [1]. These structures range in size from proteins comprising under 100 amino acids to virus particles of several million molecular weight. An area of intense interest currently concerns macromolecular complexes containing multiple components that must periodically assemble and disassemble in order to carry out their biological function.

A classic example in all higher cells is the nucleosome, which is the fundamental repeating unit of DNA organization in chromosomes and accounts for the two most fundamental levels of chromatin structure. Not only do nucleosomes efficiently package DNA, they are also intimately involved in the gene expression mechanisms that allow only selected regions of the vast store of genomic information to be read out as a consequence of signaling processes. These two functions require about 25 million nucleosomes in each human cell nucleus.

In 1984, the structure of the nucleosome core particle (NCP), the larger part of the nucleosome, was published at 7 Å resolution [2]. The x-ray data was collected before synchrotron radiation was generally available for protein crystallography by using a single detector diffractometer and a rotating anode source. The spatial resolution of this first structure was limited by the material itself as it was prepared from whole nuclear chromatin and was therefore heterogeneous in composition. Eventually, it became technically feasible to assemble NCP in the test tube from homogeneous components made individually in bacterial cells [3]. After a long period of experimentation for developing homogeneous preparations of NCP, crystals were obtained that diffracted to high resolution. Nevertheless, the Bragg intensities from these crystals are extremely weak. Fortunately, the ESRF had opened for business, and we were invited to collect full data sets at ID13 (C. Riekel, scientist in charge) just after its construction. As a result, the structure of the nucleosome core particle was published in 1997 at 2.8 Å resolution (Figure 1) [4]. At 206 kDa, the NCP is the largest and most universal protein/DNA complex solved in atomic detail.

Fig. 1: Crystal structure of the nucleosome core particle at 2.8 Å resolution. The DNA double helix (146 base pairs in two chains: turquoise and brown) is wound around the protein histone octamer (two copies each of H2A: yellow, H2B: red, H3: blue, and H4: green) in 1.65 left-handed superhelical turns. This is the form of DNA which predominates in higher living cells. The left view is down the superhelix axis. The right view is orthogonal to the superhelix and overall pseudo-twofold axis.

Our best nucleosome core particle crystals show Bragg intensities to 1.9 Å and have measurable data to 2.0-2.1 Å spacings (Figure 2). Most recently, 27 of these crystals were used to collect a data set to 2.0 Å resolution on ID9 (M. Wulff, scientist in charge). The high brightness of both ID9 and ID13 undulator beamlines enabled our crystallographic studies of the NCP at high resolution.

AT 2.8 Å RESOLUTION (ID13)

The diffraction data was measured at ID13 (beam size 100 μm x 150 μm) over a period of 2 years (~ 75 shifts) and used to produce the first high resolution image of the NCP. In order to solve the phase problem by the multiple isomorphous replacement method (MIR), recombinant DNA technology was employed to create specific attachment sites for heavy atom derivatives in the protein portion of the complex [3]. A large number of heavy atom derivatives were screened to a

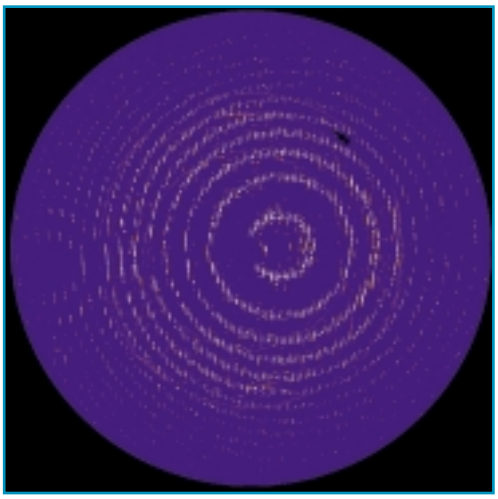

Fig. 2: Diffraction from nucleosome core particle crystals to 2.0 Å spacings. The view is nearly orthogonal to the a axis of the P212121 unit cell (108 Å x 186 Å x 111 Å). The X-ray wavelength is 0.842 Å and the crystal-to-detector distance is 320 mm. The image has been median filtered to remove the high levels of diffuse scatter.*

resolution of 4.5 Å in successive beam times, solved by difference Patterson and difference Fourier techniques, and then ranked by phasing power. Finally, one native and four derivative data sets were collected at – 170 °C to a resolution of 2.8 Å. Crystal cryo-cooling procedures were also tested and developed during these sessions at the ESRF. Because each diffraction image required 1-3 min of crystal exposure to the x-ray beam, each final data set required 3-4 crystals to keep the overall effect of radiation damage on mean intensity below 20%.

OVERVIEW OF THE STRUCTURE

The NCP contains pairs of the four core histone protein molecules named H2A, H2B, H3, and H4, and a roughly equal mass of DNA in 147 nucleotide pairs (we used 146 bp). Compared to the nucleosome, the NCP is missing only the 'linker histone' H1 and the short stretches of DNA that connect the nucleosome cores to each other in chromatin. The core histones are arranged in an octameric unit around which the DNA is wrapped in 1.65 turns of a left-handed superhelix (Figure 1) [4]. This arrangement necessitates a substantial deformation of the DNA, bending the 22 Å diameter double helix to a mean radius of 42 Å in the nucleosomal superhelix.

The histone protein chains are divided into three types of structures: 1) rigid, folded alpha-helical domains named the histone-fold, 2) histone-fold extensions which interact with each other and the histone-folds, and 3) flexible 'histone tails'. The histone-fold domains are structurally highly conserved between the four types of core histones and have also been discovered in an increasing number of other molecules involved in the regulation of gene read-out or transcription. They form crescent-shaped heterodimers which have extensive interaction interfaces in the pairings H3 with H4 and H2A with H2B. The histone-fold domains are responsible for organizing 121 base pairs (bp) of DNA in the superhelix, not the entire 147 bp. It is the responsibility of the extensions just prior to the H3 histone-folds to bind the first and last 13 bp of DNA. The flexible tails of the histones reach out between and around the gyres of the DNA superhelix to contact neighboring particles. About one-third of these flexible histone tails can be observed in the electron density map, the remainder are too disordered to be interpreted. The implication from the structure is that these flexible regions are meant to make inter-nucleosomal interactions, perhaps facilitating the formation of nucleosome higher-order structures (HOS).

PROTEIN-DNA INTERACTIONS

There are 14 regions of contact between the histone proteins and DNA: three by each of the four histone-fold dimers and two by histone-fold extensions. This construction allows the DNA molecule in a single nucleosome core to come loose over one-half of the superhelix while the histones maintain their grip on the other half, permitting the genetic information stored in the DNA to be read out without complete dissociation of the DNA from the histone octamer. The nucleosome core was previously thought to be held together simply by electrostatic attraction: the negatively charged DNA molecule wound as yarn around a positively charged histone spool. Although this type of interaction does occur, equally many interactions of other kinds, such as hydrogen bonds and hydrophobic interactions, are also important.

DNA DEFORMATION

The path of the DNA around the histone octamer deviates from that of an ideal superhelix, displaying strong bends in some regions, while being nearly straight in others. This path is determined predominantly by the histone/DNA contacts and is probably largely independent of the DNA sequence of nucleotides. The close spatial proximity of the two turns of the DNA superhelix with a pitch of 24 Å, and the periodic variation of double helix parameters with a mean of 10.3 bp per turn, result in an alignment of major and minor grooves from one superhelical gyre to the next (Figure 1).

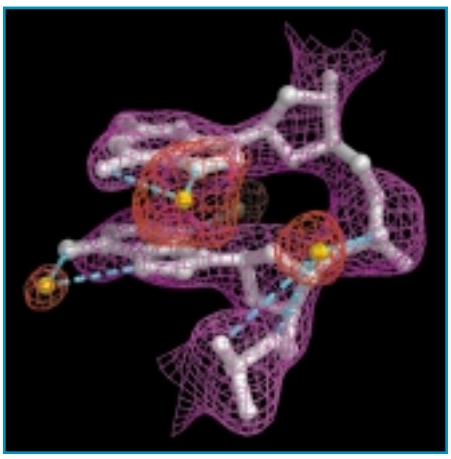

Fig. 3: Two consecutive bases of nucleosomal DNA (white) and solvent molecules (yellow). The atomic positions are based on a 2Fo-Fc electron density map (DNA: magenta, solvent: red) calculated between 47 and 2 Å resolution (contoured at 1.1 sigma). Distances between DNA and solvent molecules greater than 2.2 Å and less than 4.4 Å are shown (cyan).

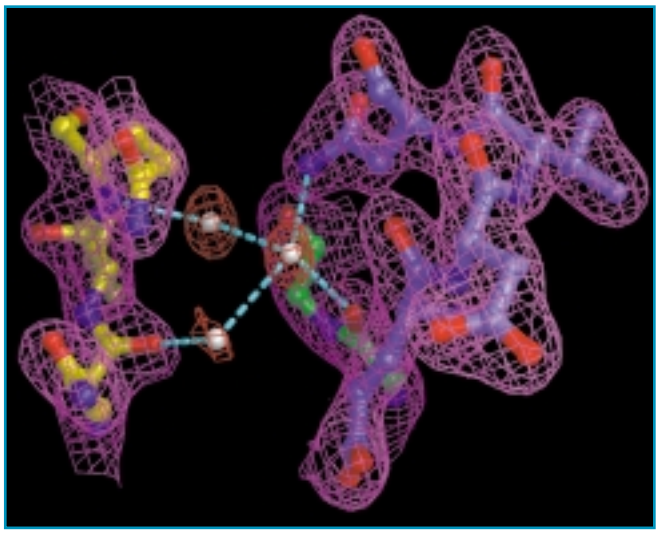

Fig. 4: Ordered solvent molecules (white) at the interface between the protein chains of histone H2A (yellow), histone H3 (blue) and histone H4 (green). Oxygen atoms are shown in red, nitrogen atoms in dark blue. Distances between protein and solvent greater than 2.2 Å and less than 3.5 Å are shown in cyan. A 2Fo-Fc electron density map, calculated as described for Figure 3, and contoured at 1.7 sigma, is shown for the protein (magenta) and for solvent (red).

The resulting narrow channels formed by the aligned minor grooves serve as the exit points for four of the eight basic histone tails, whereas the large pores formed by the aligned major grooves are, in principle, free to make base-specific contacts with other proteins. The Debye-Waller B-factors show that the mobility of the DNA backbone varies greatly, having low values when it is bound to the histone octamer and high values when it is facing away from it.

AT 2.0 Å RESOLUTION (ID9)

X-ray data to 2.0 Å resolution was collected at ID9 (beam size 150 μm x 300 μm) using a monochromatic x-ray beam and a 30 cm Mar Image Plate detector (Figure 2). Crystals of an average size of 200 μm x 200 μm x 500 μm diffracted very weakly, requiring exposure times of 90 s for each 0.4° rotation picture to record the highest resolution data. The previous observations of radiation damage incurred by these crystals despite cryo-cooling indicated the need to collect a large number of partial data sets. A total of 27 partial data sets were collected, each one covering a rotation range of 8.0° and overlapping the neighboring sets by 4.0° to accommodate crystal misalignment. Two crystal orientations with respect to the rotation axis were used to ensure coverage of the blind zone. The substantial exposure times necessary to collect the high resolution data required collection of an additional 3.0 Å resolution data set using exposure times of 10 sec to recover 'overflows'. Ultimately, the program «denzo» was used to measure a total of 4,228,118 reflections from 570 exposures and to merge them to obtain our 2.0 Å data set. The final completeness of the data is 98.3% (84.5% in the last shell: 2.04 - 1.97 Å) with an overall R-factor of 6.8% (reaching 30% in the 2.22 - 2.13 Å shell). The refinement of the structure at this resolution is currently in progress.

WATER AND IONS

The 2.0 Å diffraction data have allowed us to locate a large number of well-ordered water molecules and ions. We expect to gain valuable general information on the role of water molecules in mediating protein-DNA and protein-protein interactions. The binding of divalent metal ions, such as manganese or magnesium, to the DNA appears to favor the distortion of the DNA seen in the NCP (Figures 3 and 4). The presence of ordered water molecules at the interface between the protein subunits may provide a means to favor their disassembly and thus could be important to the processes of DNA transcription and replication.

OUTLOOK

The nucleosome core particle structure explains in atomic detail how DNA is kept untangled in the cell nucleus and clarifies the unique role of the nucleosome in maintaining and controlling the expression of genetic information. Nucleosomes do not exist as isolated particles in the cell, but are packed into arrays with an internal repeat of 157-240 bp. The dynamic assembly and disassembly of the higher-order structures made from these arrays helps determine the functional state of DNA. HOS formation is apparently guided by interactions with non-histone nuclear proteins in addition to the DNA sequence preferences displayed by the histone octamer itself. The NCP structure has already provided information that has allowed us to construct a nucleofilament zigzag structure in crystals and add a major fragment of the H1 linker histone to it. Work on this structure is currently in progress at the ESRF. Beyond this, we will endeavor to elucidate the structures of higher-order arrangements of nucleosomes in the chromatin fiber and to relate this information to the way these assemblies participate in gene regulation. ■

REFERENCES

[1] W.A. Hendrickson and K. Wüthrich, eds., Macromolecular Structures (Current Biology, London) (1997).

[2] T. J. Richmond, J. T. Finch, B. Rushton, D. Rhodes and A. Klug, The structure of the Nucleosome Core Particle at 7 Å Resolution. Nature, 311, 532-537 (1984).

[3] K. Luger, T. Rechsteiner, A.J. Flaus, M. M. Y. Waye and T. J. Richmond, Characterization of Nucleosome Core Particles Containing Histone Proteins Made in Bacteria. J. Mol. Biol., 272, 301-311 (1997).

[4] K. Luger, A.W. Mäder, R.K. Richmond, D.F. Sargent and T.J. Richmond, Crystal Structure of the Nucleosome Core Particle at 2.8 Å Resolution. Nature, 389, 251-260 (1997).

Observation of Speckle Patterns by Coherent X-ray Scattering from Thin Polymer Films

P. Müller-Buschbaum[1], T. Thurn-Albrecht[1], G. Meier[1], M. Stamm[1], E.W. Fischer[1], B. Stark[2], B. Stühn[2], D.L. Abernathy[3], G. Grübel[3]

1 Max-Planck-Institut für Polymerforschung, Mainz (Germany)
2 Fakultät für Physik, Universität Freiburg (Germany)
3 ESRF, Experiments Division

A speckle pattern is produced whenever a disordered material causes random phase shifts while scattering coherent incident light. Changes of the disordered structure with time lead to fluctuating speckle patterns. The observation of these intensity fluctuations at a single point in the speckle pattern provides a direct measure of the underlying dynamics.

In the wavelength regime of visible light this dynamic light scattering is a well-established technique [1, 2] capable of probing dynamics up to q-vectors of typically 4 x 10^{-3} Å^{-1}. This limitation has been overcome recently by correlation spectroscopy with x-rays (XPCS). Using a wide bandpath coherent x-ray beam [3], the translational dynamics of systems such as colloidal aggregates [4] or block copolymer miscelles [5] could be studied. Motivated by the observation of static x-ray speckles in block copolymer systems [6, 7], we were interested in exploring the feasibility of XPCS for the study of surface and interface dynamics. Two types of polymer samples were chosen: On one sample the diffusely scattered intensity, containing information about surface morphology, is created by an additional roughness introduced by small droplets on top of the surface (Figure 1a). The other sample of multilayer type scatters due to the density difference at internal interfaces which are strongly correlated (Figure 1b). This roughness correlation gives rise to resonant diffuse scattering, which concentrates the diffusely scattered intensity into narrow sheets in reciprocal space [8]. We show that these samples might be good candidates for measurements concerning the dynamics of surfaces, like capillary waves, by performing x-ray photon correlation spectroscopy.

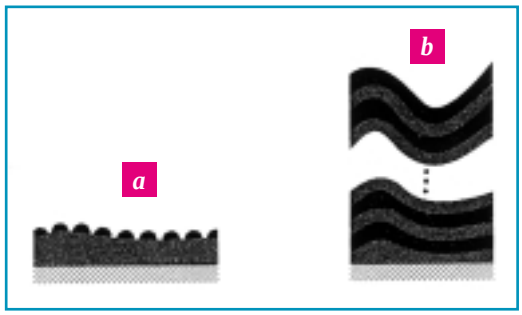

Fig. 1: Schematic drawing of the two sample types used in the coherent experiment: (a) droplets on a thin polymer blend film and (b) layered lamella of diblock copolymer (about 50 layers, not all shown).

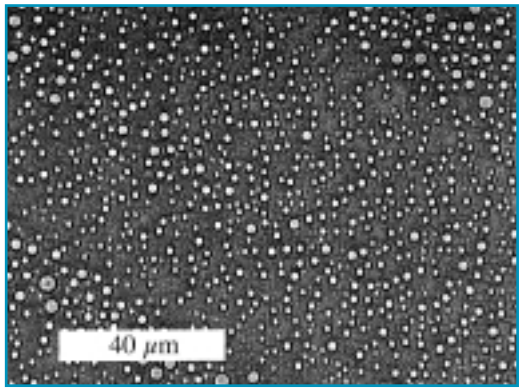

Fig. 2: Optical micrographs of the blend film sample (magnification 50 times) displaying the surface structure consisting of small droplets which were used for the surface labelling.

The experiments were performed at beamline ID10A at the ESRF using a wide bandpath set-up [3] for coherent scattering in small-angle reflectivity geometry.

Polymer blends exhibit a complex behavior upon spin-coating due to the possibility of phase separation occurring during the film formation. We used polystyrene (PS) and polybromstyrene P(Br$_x$S) with a degree of bromination of x = 0.72. Figure 2 displays an optical micrograph of the sample surface with a magnification factor of 50, displaying droplets with a mean diameter of 2 μm. They consist of PBrS in a matrix of PS. The laterally disordered domain structure is caused by the partial wetting behavior of the blend. PBrS entrapped in the PS phase during the rapid evaporation of the solvent, segregates to form droplets at the surface. In the investigated q-range, capillary waves have only little contributions compared to the contributions of the droplets, and the droplet motions on a polymer melt can be studied. With the increase of roughness the diffusely scattered intensity, which contained the information about the surface morphology [9], is increased too, providing an increased intensity for coherent experiments.

Installing the above described requirements for coherent x-ray scattering we measured the static speckle patterns by performing common 'detector-scans' (the sample is held fixed at one angle of incidence α_i and the detector angle α is varied). According to $\Delta q_x \sim \pm(2\pi/\lambda)\,\alpha\,\Delta\alpha$ and $\Delta q_z \sim \pm(2\pi/\lambda)\,\Delta\alpha$, changes in the exit angle $\Delta\alpha$ will mainly result in a change of q_z and only very small changes in q_x. Typical speckle patterns are presented in Figure 3. The exit angle equals the critical

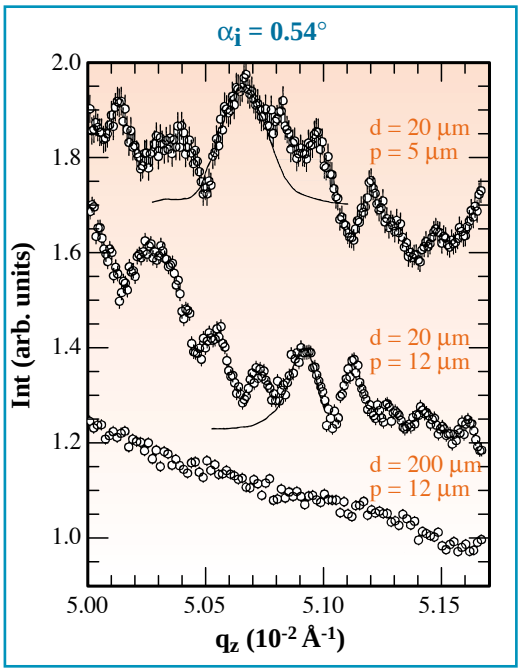

Fig. 3: «Detector-scans» measured at the angle of incidence α_i = 0.54° of the blend film sample demonstrating the influence of the front pinhole p and the detector pinhole d. In each scan the q_x value is changed between 1.69 x 10^{-4} Å^{-1} and 1.72 x 10^{-4} Å^{-1}. The solid line shows the width of the central peak of the Fraunhofer diffraction pattern as yielded by the measurement. For clarity the curves are shifted against each other.

angle of PS which corresponds to α_i = 0.54°. Therefore the measurements are performed through a Yoneda peak. The width of the speckles depends on the size of the front pinhole aperture *p*. The angular extent of each spot is comparable to that of the central peak of the Fraunhofer diffraction pattern λ/p of the pinhole. An enlarged pinhole aperture causes a narrower diffraction pattern and therefore narrower speckles. The solid lines in the two top curves (20 μm detector pinhole) show the width of the measured central peaks of the primary beam with the corresponding front pinhole for comparison. The good agreement shows that the observed intensity distribution is due to a static speckle pattern from the sample surface. Increasing the detector pinhole *d* by a factor of 10 averages out the sharp speckle structure corresponding to the observation of the ensemble averaged structure factor.

Block copolymers are interesting materials due to their particular phase separation behavior. Because of the chemical connectivity of the components only microphase separation of mutually incompatible blocks takes place. Therefore phase separation occurs only on a molecular scale. This order-to-disorder (ODT) transition is controlled by the degree of polymerisation and the Flory-Huggins segment interaction parameter. Due to selective interactions surfaces can influence the structure formed during a phase separation process. One component may segregate to the surface of the film introducing a surface-induced order. In oriented films the structures extend over large distances and for a symmetric block copolymer a lamellar ordering is induced. The characteristic periodicity d of these lamella is of the order of the radius of gyration.

For the experiments presented here, polystyrene-block-polyisoprene (PS-b-PI) with a symmetric composition was used. For the bulk material an order-to-disorder transition temperature T_{ODT} = 178 °C was obtained.

For the dynamics of such systems one expects collective interfacial modes in which adjacent interfaces move in phase. In the case of full correlation the in-plane morphology of the upper layer would equal the one of the underlying layer through the whole sample. Whereas for a sample with uncorrelated interfaces all interfaces scatter independently and the diffuse intensities of all individual interfaces superpose, the case of partially or fully correlated roughness gives rise to a coherent superposition of the contributions from individual interfaces leading to a much higher intensity. The intensity is concentrated in narrow sheets. These sheets of resonant diffuse scattering are oriented perpendicular to the q_z-axis with the center fulfilling the one dimensional Bragg-condition $\Delta q_z = 2\pi/d$ [9].

Static speckle patterns from this system were recorded by performing «detector-scans». The scans were taken around the q_z-value of the first order Bragg peak, however slightly off-peak in q_x (two times the full width half maximum of the Bragg peak) to avoid contamination of the signal from specular reflection. Again we measured a well-pronounced speckle pattern comparable to the ones of the blend sample. However they do not result from an increased intensity due to surface labeling but are due to an increased intensity by resonant diffuse scattering. Whereas at room temperature speckles are nearly independent of time, at *T* = 125 °C, above T_g of the PS-block, we observe speckle patterns fluctuating on the time scale of a few minutes.

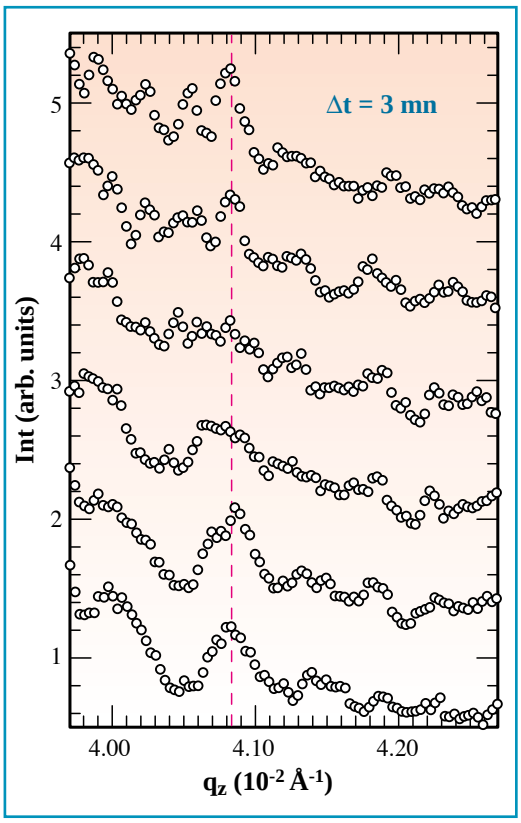

Fig. 4: Time series of «detector-scans» performed at T = 125 °C. The angle of incidence was α_i = 0.224° for the examination of the diblock copolymer film sample (p = 5 µm and detector sided pinhole aperture of 20 µm). For clarity the curves are shifted against each other. The dashed line is a guide to the eye.

As an example we show a time series of detector scans in Figure 4. Each scan was taken after three minutes delay time with a counting time of one second per point. In summary we presented experiments using coherent x-ray scattering in a reflection geometry to investigate thin polymer films. In the blend film system the scattering in the demanded *q*-range is enhanced by surface labelling, whereas in the diblock copolymer film system the roughness correlation of the multilayer interfaces provides the high intensity. Therefore both samples are well suited for experiments using x-ray photon correlation spectroscopy, because they deliver a good signal-to-noise ratio in the observed speckle patterns. Thus they are good candidates for further dynamic measurements. This will enable the determination of the time correlation function of the surface and interface dynamics and will open up the door for examinations of capillary waves, surface diffusion processes and membrane dynamics. ■

References

[1] B. Berne, R. Pecora: Dynamic light scattering; Wiley-Interscience, New York (1975).

[2] D. Langevin: Thin liquid films; in «Light scattering by liquid surfaces and complementary techniques»; edited by D. Langevin, Marcel Dekker INC., New York, 265 (1992).

[3] D.L. Abernathy, G. Grübel, S. Brauer, I. Mc Nulty, G.B. Stephenson, S.G.J. Mochrie, A.R. Sandy, N.Mulders, M.Sutton; J. Synchrotron Rad. 5, 37 (1998).

[4] T. Thurn-Albrecht, W. Steffen, A. Patkowski, G. Meier, E.W. Fischer, G. Grübel, D.L. Abernathy; Phys. Rev. Lett. 77, 5437 (1996).

[5] S.G. J. Mochrie, A.M. Mayer, A.R. Sandy, M. Sutton, S. Brauer, G.B. Stephenson, D.L. Abernathy, G. Grübel; Phys. Rev. Lett. 78, 1275 (1997).

[6] G. Vignaud, G. Grübel, A. Gibaud, D. Auserre, J.F. Legrand; ESRF Highlights 1994/1995, 8.

[7] Z.H. Cai, B. Lai, W.B. Yun, I. Mc Nulty, K.G. Huang, T.P. Russell, Phys. Rev. Lett. 73, 82 (1994).

[8] V. Holy, T. Baumbach; Phys. Rev. B 49, 10668 (1994).

[9] S.K. Sinha, E.B. Sirota, S. Garoff,

First Experiments on Troïka II

D.M. Smilgies, N. Boudet and G. Grübel

ESRF, Experiments Division

The Troïka II beamline (ID10B) started user operation on schedule in April 1998. This second branch of the Troïka beamlines is again an open beamline with a flexible diffractometer which aims at providing additional beam time for demands in the soft-condensed matter community. Special emphasis to surface and interface studies using grazing-incidence diffraction and x-ray reflectivity is given.

Although Troïka II uses the same undulator source as Troïka I (ID10A), both stations can work independently in parallel. A thin diamond (111) crystal acts as monochromator and beam splitter (see Figure 1), a technique which has been pioneered at the Troïka beamline. A second (111) diamond crystal deflects the monochromatic beam at a constant offset from the white beam path. The energy range of this double-crystal monochromator is 8 to 12 keV. As a further optical element, a plane double mirror for harmonic rejection is in preparation. Presently, harmonic rejection is achieved with two small mirrors in the experimental hutch.

The Troïka II eight-circle diffractometer with an additional beam deflector can operate both in horizontal and vertical scattering geometry. In horizontal geometry heavy and bulky sample environments can be handled. In combination with the deflector, a device that employs either a mirror or a Bragg crystal to deflect the beam out of the horizontal plane, the horizontal geometry

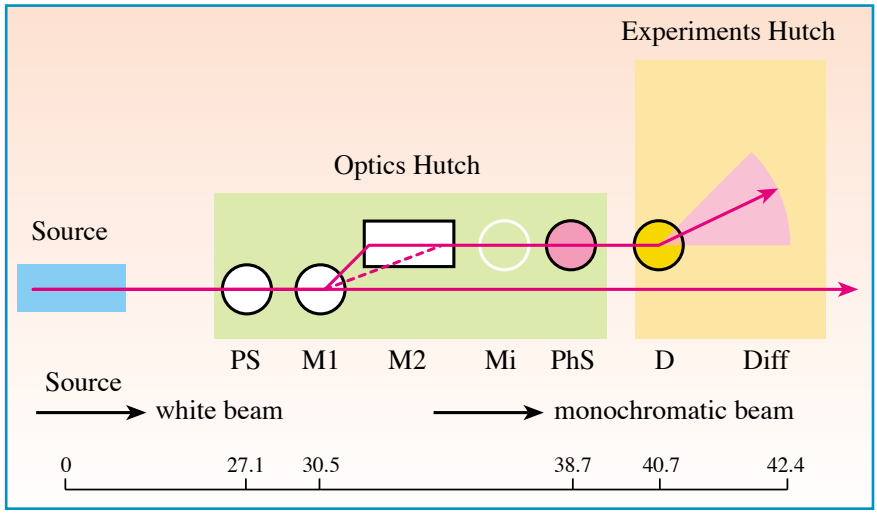

Fig. 1: Troïka II layout: PS primary slits; M1, M2 diamond double-crystal monochromator; Mi planned double mirrors; PhS photon shutter, D deflector, Diff: eight-circle diffractometer.

is particularly useful for the investigation of liquid surfaces and self-organization of amphiphilic molecules at the air-water interface. For these studies a large linear detector can be used in combination with Soller slits or an analyzer stage. In collaboration with a group at Saclay a large multi-purpose Langmuir trough is in development. Other possible sample environments could involve cryostats, furnaces, or small vacuum chambers to be supplied by the users.

The vertical scattering geometry is used for small samples and sample environments to study surfaces or thin films in air or under inert gas. In this geometry the largest reciprocal space access is provided. It will be particularly important for the in-house research activities which will focus on the investigation of thin organic films on solid substrates. Various detector options are available, such as a scintillation detector with motorized slits and a small linear detector which can be combined with an analyzer stage.

The spectrum of research activities at Troïka II can be best exemplified by the first six user experiments. In the very first experiment, Daillant *et al* investigated the diffuse scattering from the surface of water and various other liquids. The goal of the experiment was to determine whether there are higher order corrections to the surface tension. In the experiment the incident x-ray beam impinges on the liquid surface below the critical angle and creates an evanescent wave parallel to the liquid surface with a penetration depth of about 50 to 100 Å. The evanescent wave is scattered by capillary waves giving rise to diffuse scattering up to 50° scattering angle in-plane which is integrated perpendicular to the liquid surface by a large linear detector. Important for this experiment is a very clean, well defined beam without high-energy contamination. The latter was achieved by a low-pass filter consisting of two small platinum coated mirrors in deflector and flight path which were set close to the critical angle.

In the second experiment, Möhwald *et al* characterized selected phases in the phase diagram of the fatty acids $C_nH_{2n+1}COOH$ with n = 18, 20, 22, and 24. The phase diagram of these amphiphilic molecules is well understood theoretically and certain predictions were to be tested in the experiment. In particular, the variation of the lineshapes in the L_2 to L'_2 phase transition was to be investigated where the direction of the tilt of the molecular axis changes from the nearest-neighbor direction to next-nearest neighbor. The data are presently being analyzed.

The remaining four experiments use the vertical scattering geometry. Lacaze *et al* tried to determine the 4 x 16 phase of the liquid crystal 8CB absorbed on MoS_2 which they found previously with STM and first grazing-incidence diffraction experiments. This experiment is very difficult due to the large mosaicity of about 0.5° of the substrate and the low Z of the liquid crystal film. The experiment addresses the problem of anchoring a liquid crystal on an atomically well-defined interface. In the following experiment by Lucas *et al* the electrochemical absorption of CO on Pt(111) and Pt(100) surfaces will be studied. Again the problem will be to see a low-Z monolayer on a high-Z substrate. Finally, the last two experiments by Abstreiter *et al* and Metzger *et al* will investigate the self-organization of quantum dot arrays in strain-modulated superlattices. In these last two experiments a high-resolution set-up with analyzer and linear detector will be used.

The Troïka II beamline addresses the needs of both the soft and hard-condensed matter community by making more beam time available for interface and thin films studies. A variety of scattering geometries and detectors options is available. For more detailed information, please contact D. M. Smilgies (tel +33 (0) 4 76 88 27 31 – email: smilgies@esrf.fr).

Hierarchical Porosity in Quasicrystals Investigated by Coherent X-ray Imaging

L. Mancini[1,2], J. Gastaldi[1], E. Reinier[1], P. Cloetens[2,3], W. Ludwig[2], C. Janot[4,6], J. Härtwig[2], M. Schlenker[5] and J. Baruchel[2]

1 CRMC2-CNRS, Marseille (France)
2 ESRF, Experiments Division
3 EMAT-RUCA, Antwerp (Belgium)
4 Dip. Scienze della Terra, Univ. 'La Sapienza', Roma (Italy)
5 Laboratoire Louis Néel, CNRS, Grenoble (France)
6 Laboratoire de cristallographie, CNRS, Grenoble (France)

An unexpected kind of solids, the quasicrystals, with long range translational order but no periodicity, was discovered in 1984 [1]. A lot of effort was devoted, from that moment, to understand their peculiar properties, in particular their growth mechanism and stability.

The observation, by hard x-ray phase imaging [2-4] and phase microtomography [4,5], of oriented dodecahedral holes, located in the bulk, of high-quality, centimetre-size, single grain icosahedral AlPdMn quasicrystals, is considered by the scientific community concerned as a crucial result. It was made possible by the high spatial coherence of the beam at the «long» (145 m) ID19 beamline. Figure 1 shows one of the central results: the sizes of the observed holes display a discrete distribution, with peaks at 22, 5 and slightly more than 1 μm. Gas bubbles would lead to a continuous distribution. The jump from one size to the next corresponds to the factor τ^3, where τ is the golden mean ($\tau = 2 \cos 36° = 1.62$), a basic ingredient in all theoretical approaches of quasicrystals. The three-dimensional reconstruction resulting from phase microtomography shows that the average distance between neighboring holes is, again, about τ^3 times the hole size (Figure 2).

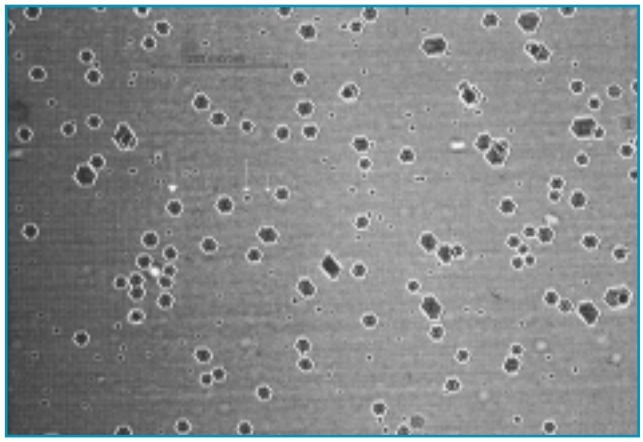

Fig. 1: Phase radiography of an AlPdMn quasicrystal (sample-to-detector distance 50 cm, λ = 0.35 Å) showing three families of dodehahedral holes (arrows).

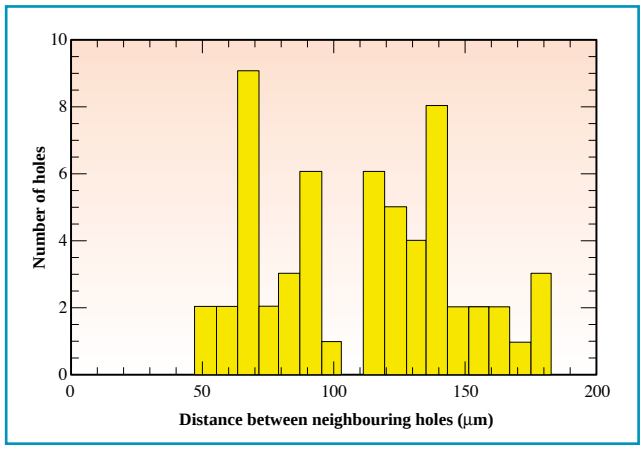

Fig. 2: Three-dimensional reconstruction resulting from a phase microtomography (sample-to-detector distance 50 cm, λ = 0.52 Å) of an AlPdMn quasicrystal, showing the holes locations.

Figure 3 shows that annealing alters the shape and sizes of the holes and reduces their number. The discrete distribution of sizes flattens out and changes gradually into a continuous one. It was often observed that lamella-shaped crystalline inclusions form in the neighborhood of the holes.

Figure 4 shows a diffraction image («topograph») and a phase image corresponding to a hole. The topograph shows a white-black contrast which indicates that a gradient of distortion is present in the hole neighborhood. This contrast can be simulated by simply assuming, as a first approximation, that the deformation field is similar to the classical one around a spherical inclusion in a crystal [4].

The features observed on as-grown grains could support the predictions of a model which describes the quasicrystal structure in terms of a hierarchical self-similar packing of overlapping atomic clusters. An inflation scale factor τ^3 preserves long-range order but generates a hierarchy of holes and a fractal structure. The observations appear to be in fair

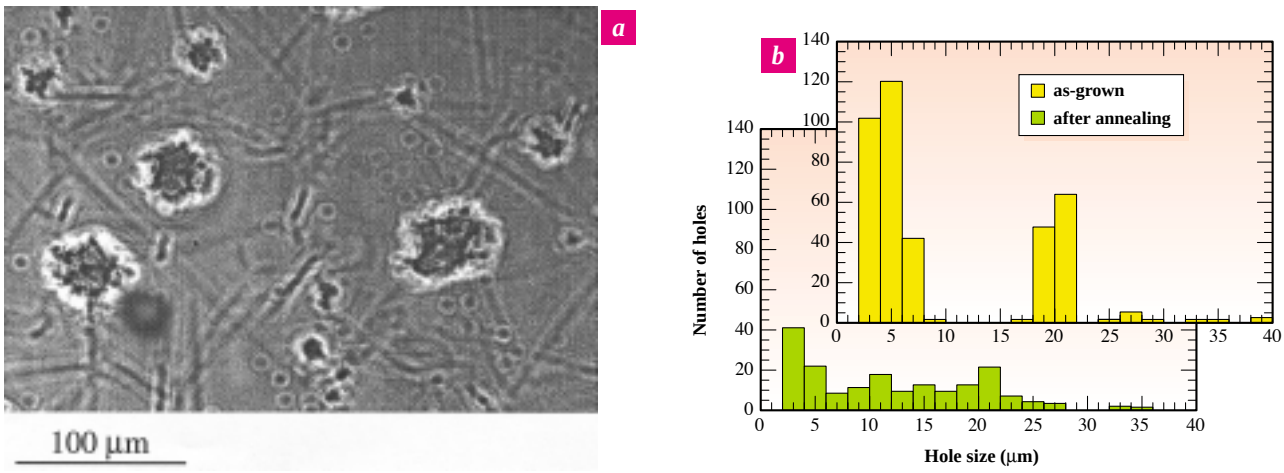

Fig. 3: Phase radiography after an annealing treatment showing deformation of the hole shapes and the appearance of lamellas of a crystalline phase.

agreement with these predictions [6], albeit with no indication about holes with size below the experimental resolution limit of about 1 μm, and with lower volume fractions and a flattened hierarchy. This flattening could result from the quasicrystal single grains having effectively, because of their low thermal conductivity, suffered annealing even in their as-prepared state. But the lower volume fractions of holes clearly indicate that the present model is not a final point. Systematic experiments are being performed to further clarify this topic. ■

REFERENCES

[1] D. Schechtman, I. Blech, D. Gratias, J.W. Cahan, Phys. Rev. Lett. 53, 1951 (1984).

[2] L. Mancini, E. Reinier, P. Cloetens, J. Gastaldi, J. Härtwig, M. Schlenker, J. Baruchel, Phil Mag.A, in press.

[3] E. Reinier, PhD Thesis, Univ. Aix-Marseille (1998).

[4] L. Mancini, PhD Thesis, Univ. J. Fourier, Grenoble (1998).

[5] W. Ludwig et al., to be published.

[6] L. Mancini, C. Janot, L. Loreto, R. Farinato, J. Gastaldi, J. Baruchel, Phil. Mag. Lett., vol 78, n° 2, 159-167 (1998).

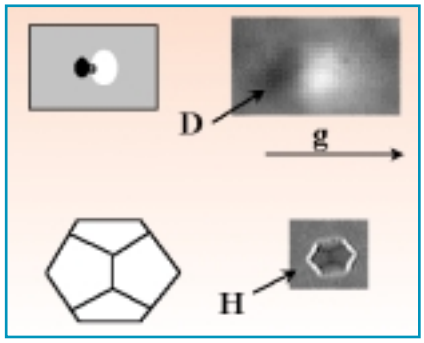

Fig. 4: a) diffraction and b) phase image of a hole; the diffraction image shows that the presence of a hole is associated with a distortion of the quasicrystal in its neighborhood.

WHAT ARE QUASICRYSTALS ?

Quasicrystals are solids which have a new type of long-range order, such that their diffraction patterns show Bragg reflections revealing symmetries which are incompatible with periodicity (five-fold or ten-fold axis, for instance). Large single grains can be grown for some of the quasicrystalline alloys, like AlPdMn. Their quality is such that dynamic diffraction effects have been observed. Quasicrystal structures can be described in different ways. One of them consists in filling with atoms an appropriate quasiperiodic tiling, produced from two basic tiles and matching rules (Fibonacci chain in 1D, Penrose tiling in 2D,...). Another approach involves only one basic unit (a cluster of atoms) and a replication process; it implies some overlaps and holes.

In a higher dimensional space it is possible to describe the 3D-quasiperiodic structure as a periodic one. The actual quasiperiodic structure in the 3D-physical space is obtained from the hyperspace structure by an appropriate projection/section technique. The Bragg peaks observed on the AlPdMn quasicrystals, for instance, can be indexed in a 6D periodic hyperspace.

Aside from their peculiar structure, quasicrystals also exhibit very unexpected properties. This includes very high electrical and thermal resistivities: quasicrystals are therefore insulator alloys containing about 70% of aluminium! Other interesting properties involving, for instance, adhesion, corrosion, friction, and hardness suggest that quasicrystals are promising materials for industrial applications, particularly coatings.

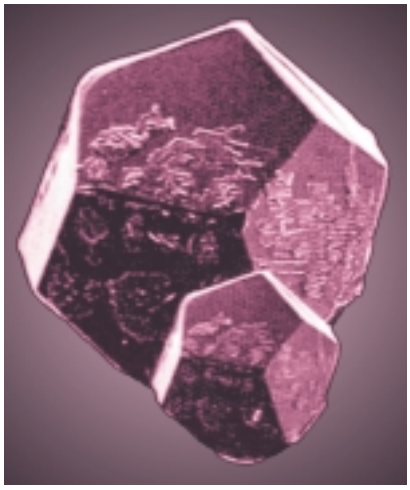

Reference

See, for instance, C. Janot, «Quasicrystals: a primer», Oxford Univ. Press, 2nd edit. (1994)

ID26 : X-RAY SPECTROSCOPY ON ULTRA-DILUTE SYSTEMS

CH. GAUTHIER, V.A. SOLÉ, J. GOULON, E. MOGUILINE AND R. SIGNORATO

ESRF, EXPERIMENTS DIVISION

The ESRF beamline ID26 is dedicated to x-ray absorption spectroscopy on ultra-dilute systems (XAUS) in the spectral range 2.3 - 30 keV. The aim of the beamline is to extract structural and electronic information on dilute samples for which the concentration of the absorbing element ranges from a few ppm up to 10 000 ppm.

A wide range of applications is covered in biology, catalysis, chemistry, environmental sciences, solid state physics... The beamline accepted the first users in November 1997. We give herein a brief description of the beamline and we report on recent instrumentation developments.

The x-ray source consists of three phasable planar undulators. Each of them has a magnetic period of 42 mm and a length of 1.65 m. The energy of the fundamental harmonic is 2.35 keV at the minimum gap value (16 mm). The whole energy range is obtained by exploiting different harmonics of the undulators emission spectra. The design of the beamline optics is optimized in order to reduce background radiation and to provide an efficient harmonic rejection. The first component is a flat silicon mirror that deflects the beam laterally apart from the bremsstrahlung emission cone of the ring. This mirror damps the thermal power of the x-ray source and protects the other optical components. The x-ray beam is focused by two segmented piezoelectric bimorph silicon mirrors in a Kirkpatrick-Baez configuration, which are located in the monochromatic section of the beamline. The typical focal spot size at the sample location is 200 μm (horizontal) x 15 μm (vertical). The photon flux on the sample is 10^{13} photons per second. Smaller spot size could be achieved (H : 80 μm x V : 7 μm) with a lower flux (10^{12} photons/s). Each mirror has three reflective layers: silicon, chromium and platinum.

A two-crystal fixed-exit Kohzu monochromator is inserted after the first horizontally deflecting mirror. The monochromator is equipped with two pairs of crystals Si (111) and Si (220) cooled down to - 140 °C. The crystal pairs can easily be exchanged using a lateral translation of the monochromator.

Two experimental stations are used: a small fluorescence chamber operated at room temperature and a fluorescence station equipped with a continuous flow liquid helium cryostat. The temperature range covered goes from 4.8 K to 293 K. The cryostat is equipped with a very accurate (1 μm) vertical sample translator and a rotary stage with an angular accuracy of 0.13 mrad.

XAS spectra are recorded in the fluorescence excitation mode. To reach high dilution, three main difficulties had to be overcome : **i)** The fluorescence signal is usually buried into a large radiation background (mainly elastic or inelastic scattering) originating from sample matrix. One has to get rid of this background which degrades the fluorescence signal statistics. **ii)** Since the narrow emission peaks of the undulator spectra (typ 100-200 eV) are not suitable to record a whole EXAFS scan, we had to extend the gap scan techniques recently developed at the ESRF [1]. **iii)** Due to the very high flux delivered at the ID26 beamline, sample radiation damage is usually a major source of difficulties, especially in the case of biological samples. In order to overcome these difficulties, different data acquisition strategies have been developed.

Fig. 1a: EXAFS spectrum of a 7 mMol/l Carbonmonoxy-Myoglobin sample recorded at the Fe K-edge measured in one scan of 10 seconds.

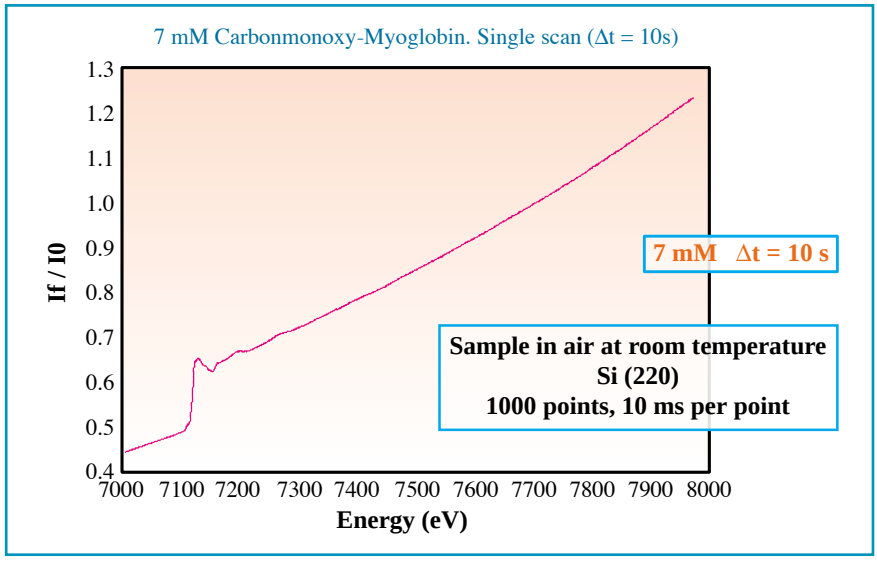

CONTINUOUS OR QUICK EXAFS FOR MODERATE DILUTIONS

For absorber concentrations above 1 mMol/l (50 to 500 ppm depending on sample matrix), the fluorescence detection is performed using silicon PIN photodiodes operated in the photovoltaic mode. The diodes are associated with a low noise current to voltage amplifier and then to a high linearity voltage to frequency converter [2]. The output signal is fed into a gated integrator (ESRF VDL

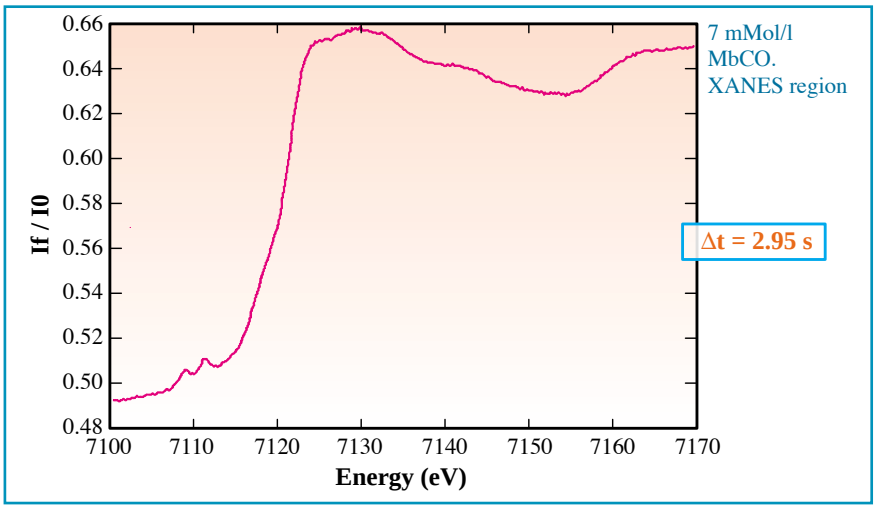

Fig. 1b: XANES region of a 40 second EXAFS scan of 7 mMol/l Carbonmonoxy-Myoglobin sample. The (220) crystal pair of the monochromator was used. The data acquisition for the XANES region is less than 3 seconds.

board). The diode can be operated with absorption filters in order to minimize the amount of background radiation reaching the detector. The IO intensity monitor is also a silicon diode associated with a scattering or fluorescence foil in an optimized geometry which minimizes the sensitivity to the x-ray beam instabilities. We take full advantage of the high saturation level, high linearity and low noise of silicon diodes which allows us to accept the very high flux delivered by the source. In the continuous gap scan technique, the monochromator Bragg angle and the undulator gap are scanned simultaneously during the measurement of the EXAFS spectra. Excellent performances were achieved: Figure 1a reproduces the EXAFS spectrum of a 7 mMol/l myoglobin sample measured in 10 seconds. Figure 1b shows the XANES part of the same EXAFS spectrum but recorded in 40 seconds. The data acquisition time of the XANES spectra was less than 3 seconds.

Averaging on several spectra indeed improves the signal-to-noise ratio. The main advantage is that radiation damage can be minimized by displacing the sample after each scan. Alternatively, the evolution of fragile samples can be monitored on a short time scale. Furthermore, there is some possibility to perform time-resolved experiments on dilute samples with a slow time evolution.

SILICON DRIFT DETECTORS

For higher dilution, it is necessary to discriminate in energy the fluorescence from the radiation background. Due to the severe counting rate limitations of energy resolving detectors, the development of large arrays of detectors (up to 100 channels) is mandatory in order to restrict the data acquisition time within realistic limits. Over recent years, we have developed new energy resolving detectors: Silicon Drift Diodes (SDD) [3]. These detectors feature a very small readout capacitance which is independent on the active area. This results in the possibility of preserving good energy resolution together with high counting rates. These detectors are associated to multichannel digital shaping amplifiers designed at the ESRF. There are clear advantages in favor of this technology: **i)** The output rate can be improved in comparison with analog shaping amplifiers. **ii)** The cost per detection channel is much lower. **iii)** The set-up of the detector array is controlled by software and can be automated. A first prototype array (12 channels) has been evaluated at the beamline. Figure 2 shows an EXAFS spectrum recorded from a 200 μmol/l aqueous solution of cobalt acetate (cobalt concentration 12 ppm) during a test experiment. The data acquisition time was 9 hours, the signal to noise ratio can be improved with longer data acquisition times. At present the highest dilution which can be achieved is 5-10 ppm depending on the absorber and the sample matrix composition. A 35 channel SDD array is under production in collaboration with Eurisys Mesures Inc. and should be operational by September 98. We expect to be able to lower the dilution limit down to 1-5 ppm. ■

Fig. 2: XAS spectrum of an aqueous solution of cobalt acetate recorded at room temperature in air with a 12 channel SDD array. The sample dilution was 200 µmol/l (12 ppm cobalt concentration). Data acquisition time was 9 hours.

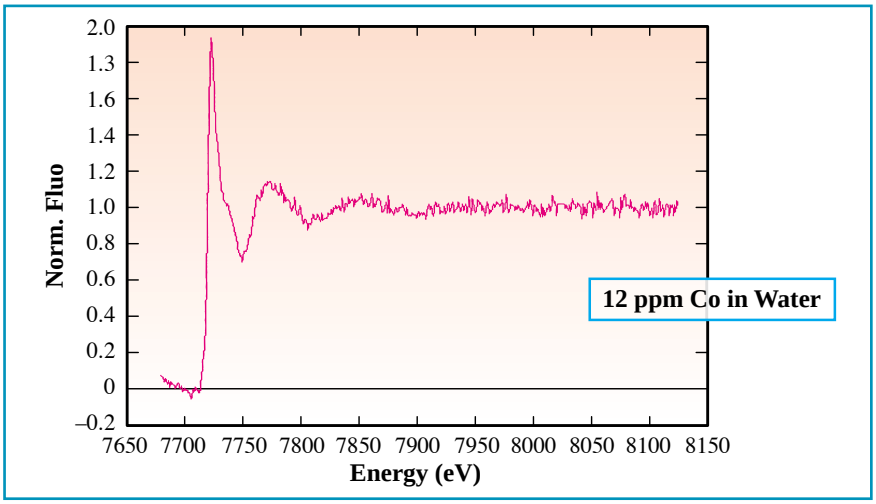

REFERENCES

[1] A. Rogalev, V. Gotte, J. Goulon, C. Gauthier, J. Chavanne and P. Elleaume. J. Synchrotron Rad. (1998) 5, 989.

[2] C. Gauthier, G. Goujon, S. Feite, E. Moguiline, L. Braicovich, N.B. Brookes, J. Goulon. Physica B208&209 (1995) 232-234.

[3] E. Moguiline, Ch. Gauthier, G. Goujon, J. Goulon, M.O. Lampert, P. Dressler, R. Henck, J. Phys. IV France7 (1997) C2 339-340.

ACKNOWLEDGEMENT

The authors wish to thank F. Natali for providing the Carbonmonoxy-Myoglobin sample.

EDGE SEPARATION USING DAFS

B. RAVEL[1], C.E. BOULDIN[1], H. RENEVIER[2], J.L. HODEAU[2] AND J.F. BERAR[2]

1 NIST CERAMICS DIVISION, GAITHERSBURG MD (USA)
2 LABORATOIRE DE CRISTALLOGRAPHIE, CNRS-UJF, GRENOBLE (FRANCE)

We exploit the crystallographic sensitivity of the diffraction anomalous fine structure (DAFS) measurement to separate the fine structure contributions of different atomic species with closely spaced resonant energies. In $BaTiO_3$ the Ti K-edge and Ba L_{III} are separated by 281 eV, or about 8.2 inverse angströms, which severely limits the information content of the Ti K-edge signal. Using the site selectivity of DAFS we can separate the two fine structure spectra using an iterative Kramers-Kronig method, thus extending the range of the Ti K-edge spectrum.

Recent x-ray absorption spectroscopy (XAS) studies [1] of the Ti *K*-near-edge and Ba K-extended spectra of $BaTiO_3$ demonstrate that the local structure in this material remains disordered even at temperatures well above the transition to a crystallographically cubic phase. The analysis of the Ti *K*-edge extended spectrum was hindered by the presence of the nearby Ba L_{III} absorption edge at 5247 eV, compared to 4966 eV for the Ti *K*-edge. This separation of 281 eV, or about 8.2 $Å^{-1}$, places such a severe limit on the information content of the Ti extended spectrum that meaningful analysis of those data is not possible. Use of an energy discriminating detector in a fluorescence XAS measurement is precluded by the proximity of the various Ti and Ba fluorescence lines. In this article we present Diffraction Anomalous Fine Structure (DAFS) as a solution to the problem of overlapping edges. DAFS has been used to separate the fine structures of single atomic species in multiple crystallographic sites, for example the Cu in $YBa_2Cu_3O_7$ [2] and the Fe in $BaZnFe_6O_{11}$ [3] or at the interfaces of a multi-layer compound [4]. Using similar methodology, we can separate the signals from the Ti and Ba sites in $BaTiO_3$, thus isolating the Ti *K*-edge fine structure spectrum and extending it beyond the 8.2 $Å^{-1}$ limit of the absorption experiment.

In the DAFS experiment, the variation in energy of the intensity of a diffraction peak is measured in an energy range spanning one or more absorption energies in the sample. The data were taken at the ESRF beamline BM2 on a 1000 Å thick film of $BaTiO_3$ deposited on sapphire by pulsed laser deposition. The film was found by x-ray diffraction to be oriented with an an axis normal to the surface. In our experiment, we measured the (100) and (200) reflections (Figure 1).

The oscillatory fine structure seen in the data above the absorption energies contains the same local structural information as an XAFS spectrum. This diffracted intensity can be expressed [2] as eq. (1):

$$I(\vec{Q},E) = \left| \sum_j M_j e^{i\vec{Q}\cdot\vec{R}_j} \left(f_j^0(\vec{Q}) + f_j'(E) + if_j''(E) + [\Delta f''(E)\tilde{\chi}(E)]_j \right) \right|^2 \quad (1)$$

where the sum is over all sites *j* in the unit cell, M_j is the thermal factor at site j, f^o is the Thomson scattering of the atom at site j, and *f'* and *f"* are the energy-dependent atomic anomalous corrections. The final term contains the complex fine structure $\tilde{\chi}$ (of which only the imaginary part is measured in a XAS experiment), as a coefficient of Δf", the portion of *f"* being due to the resonant electron.

We extracted the imaginary component of the scattering factor from the spectra of the (100) and (200) reflections. We solved eq. (1) for its real part and

Fig. 1: Measured DAFS spectra of the (100) and (200) reflections from $BaTiO_3$. The (200) spectrum is displaced upwards for clarity.

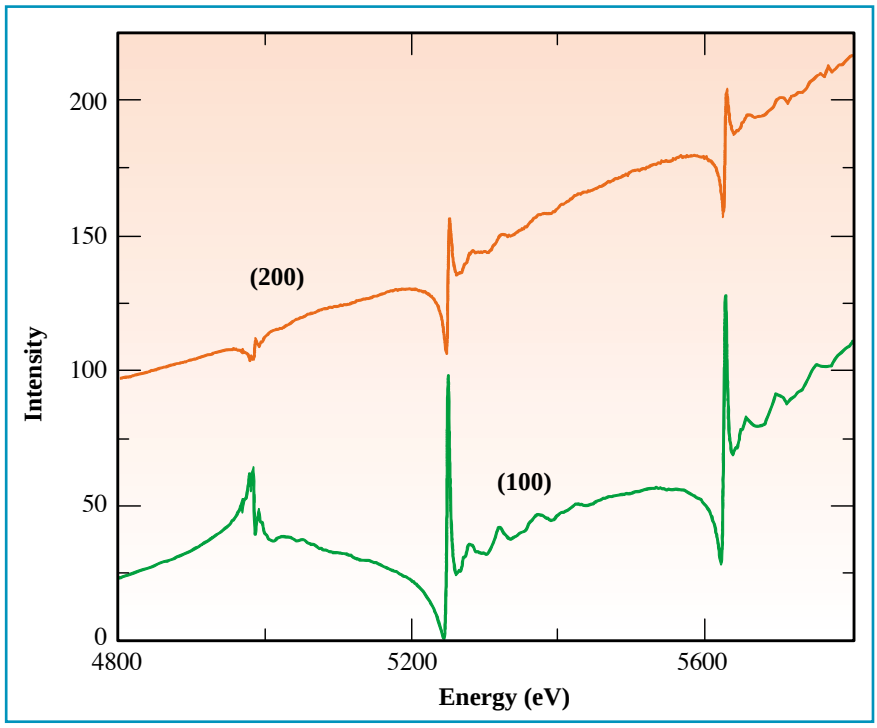

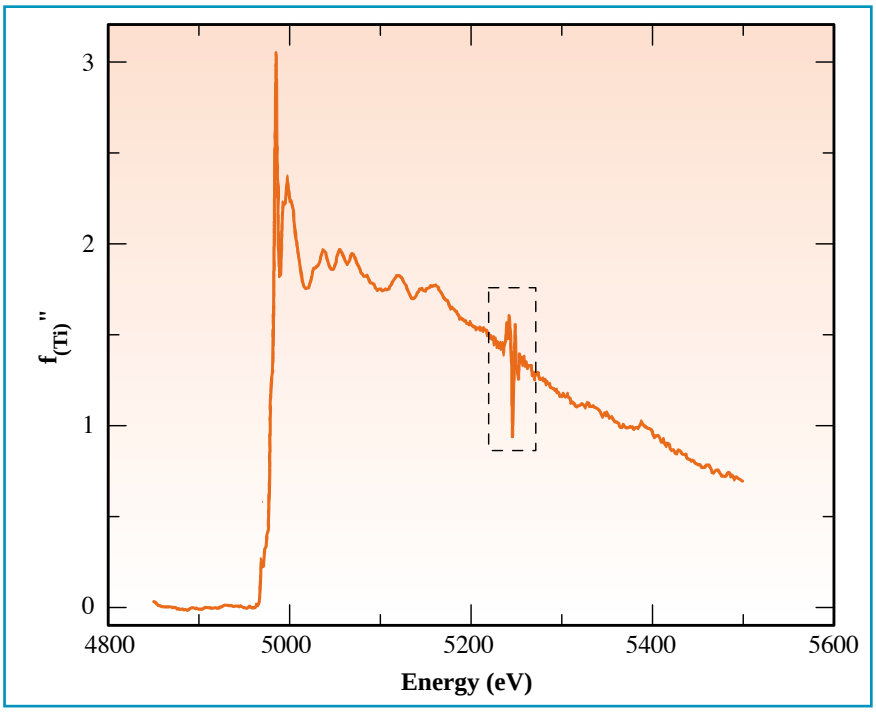

Fig. 2: Extracted f" (E) for the Ti atom. Note the incomplete cancellation of the Ba L_{III} white line at about 5250 eV.

Kramers-Kronig transform this to obtain a new value for its imaginary part [5]. The steps of solving eq. (1) and transforming are iterated to convergence. A weighed sum of the *f"* spectra are then made to yield the isolated Ti *f"* spectrum shown in Figure 2. A method developed for isolating χ" from the XAS μ [6] was applied directly to the Ti *f"* spectrum. The extracted χ" function is shown in Figure 3 along with a FEFF [7] simulation using previously-determined structural parameters [1]. The incomplete cancellation of the Ba white line results in a problem in the data which resembles a monochromator glitch. Despite this, measurable Ti fine structure signal is seen in χ between 9 and 10 $Å^{-1}$.

Using DAFS to separate the fine structures of overlapping absorption edges is a novel approach to this problem which does not require the use of energy discriminating detectors. We have shown that it yields data that is analyzable beyond the second absorption edge energy. There are many transition metal/rare-earth compounds of technological interest which are composed of atoms with overlapping edges. We plan to test our method on one such material, $Gd_3Fe_5O_{12}$, a material used in microwave wave guides. In that case, the Fe K and the Gd L_{III} are separated by only 130 eV and their major fluorescence lines are separated by about 100 eV. ■

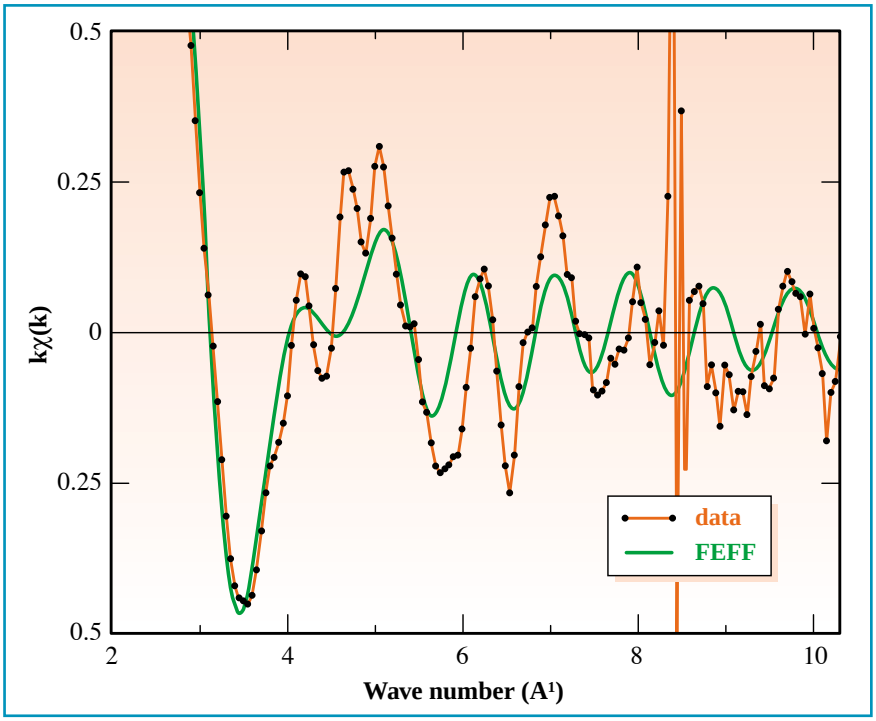

Fig. 3: χ" for the Ti atom compared to a simulation using FEFF [7]. The large feature around 8.5 $Å^{-1}$ is due to the incomplete cancellation of the Ba L_{III} white line.

References

[1] B. Ravel, E. A. Stern, R. I. Vedrinskii, and V. Kraizman. Ferroelectrics, 206-207:407-430 (1998).

[2] L.B. Sorenson, J.O. Cross, M. Newville, B. Ravel, J.J. Rehr, H. Stragier, C.E. Bouldin, J.C. Woicik, in Resonant Anomalous X-ray Scattering: Theory and Applications, edited by K. F. G. Materlik, C.J. Sparks (North Holland, Amsterdam, 1994).

[3] J. Vacinova, J.L. Hodeau, P. Wolfers, J.P. Lauriat, E. Elkaïm, J. Synchrotron Rad. 2, 236 (1995).

[4] H. Renevier, J.L. Hodeau, P. Wolfers, S. Andrieu, J. Weigelt, and R. Frahm. Phys. Rev. Lett., 78(14):2775-2778 (1997).

[5] J.O. Cross, M.I. Bell, M. Newville, J.J. Rehr, L.B. Sorenson, C.E. Bouldin, G. Watson, T. Gouder, and G.H. Lander. Phys. Rev. B (1998) to be published.

[6] M. Newville, P. Living, Y. YYacobi, J.J. Rehr, and E.A. Stern. Phys. Rev. B, 47(21):14126-14131 (1993).

[7] S. I. Zabinsky, J. J. Rehr, A. Ankudinov, R. C. Albers, and M. J. Eller. Phys. Rev. B, 52(4):2995-3009 (1995).

ACKNOWLEDGEMENTS

We thank A. Carter for providing the $BaTiO_3$ thin film sample. We also thank J.O. Cross for inspirational conversation and M. Newville for kindly supplying source code for the differential Kramers-Kronig transform. This work was supported in part by the National Research Council.

Coupling Electrochemistry with X-ray Absorption Spectroscopy to Study Polymers

P.L. Vidal[1], M. Billon[1], B. Divisia-Blohorn[1], G. Bidan[1], J.M. Kern[2], J.P. Sauvage[2] and J.L. Hazemann[3]

1 DRFMC / SI3M / LEMSI, CEA Grenoble (France)
2 Institut Le Bel, Université L. Pasteur, Strasbourg (France)
3 Laboratoire de Cristallographie, CNRS, Grenoble (France)

The field of chemically modified electrodes has seen an important growth in the two last decades, especially conjugated polymers including redox-active transition metal centers for their potential applications in electrocatalysis, sensor or electronic devices. However, there is limited information on the structure of these layers. On the other hand, x-ray absorption spectroscopy represents a highly sensitive tool to study atomic and molecular details of non-crystalline materials. Thus, EXAFS measurements on chemically modified electrodes under different controlled potentials can provide information about interactions between redox active metal centers and the conjugated structure, i.e. about the degree of electronic communication between them.

By using thiophene or pyrrole derivates bearing functionalities (a metal ion binding site, an anionic or cationic site) as monomers for electropolymerisation, electrodes can be modified with a conductive matrix containing these groups and thus can be useful in electrocatalysis, sensor or electrochromic devices. A few years ago, G. Bidan (CEA-Grenoble), J.-P. Sauvage (Univ. of Strasbourg) and co-workers have used electropolymer-isation of pyrrole-bearing 1,10-phenanthroline tetrahedral complexes of transition metals to modify electrodes, leading to sites rigidly anchored within the polymer matrix and then to stabilisation of unusual oxydation states. More recently, related works, with polythiophene, have been published by us [1] and others, in an effort for a more direct electronic coupling between the receptor site and the conjugated polymer backbone and for a better control of the structure.

By combining the phenanthroline containing macrocycle **2** with the key ligand bearing two pendant bithiophene units **1** (Figure 1) *via* the templating copper (I) ion, rotaxane complex was obtained and then electropolymerised to afford a coordinating polyrotaxane with a conjugated backbone alternating quaterthiophene moieties and phenanthroline complexes with threaded cyclic units. By testing this system for transition metal ion sensing ability, we discovered an original structural effect: as shown in Figure 2, the Cu(I) template used to assemble the fragments of the precursor could be removed but, interestingly, subsequent remetallation was only possible if lithium was present during demetallation. The function of lithium is assumed to be that of an ionic scaffolding, maintaining the topography of the coordination site after copper removal, though forming a labile complex. XAS studies at the Cu K-edge have been undertaken on this conjugated polyrotaxane at the ESRF, on the CRG-IF BM32 beamline, in order to obtain 1) information about interactions between redox active copper centers and the conjugated structure at different controlled potentials and 2) additionally proof of the high reversibility of copper(I) binding when lithium is present. The high flux available at the ESRF allows short acquisition time and due to the high dilution of metallic sites in our samples, data were collected with a highly sensitive

Fig. 1: The monomers.

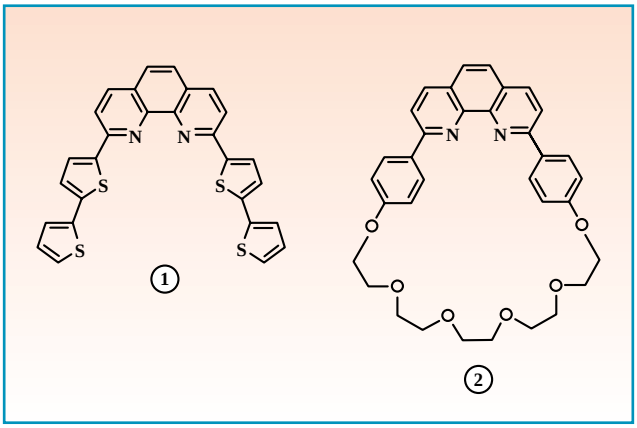

Fig. 2: Schematic representation of the synthetic strategy used and of the scaffolding effect.

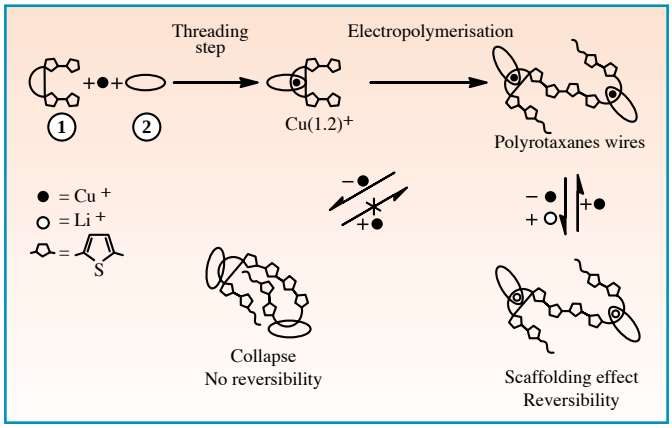

fluorescent detector. We have recorded spectra of the films of polyrotaxane electropolymerised onto a carbon electrode and in contact with a dichloromethane / 0.2M tetra-n-butyl ammonium hexafluorophosphate solution at different controlled potentials. As shown in Figure 3, changes in oxidation state of the copper centers are evidenced by the shift (by about 2.5 eV) in the position of the edge upon oxidation of the polymer film from Cu(I) (+ 0.3 V) to Cu(II) (+ l.15 V). Furthermore, no increase in the coordination number seems to occur (via a couterion in electrolyte solution) when passing from Cu(1) to Cu(II), contrary to what is observed with monomeric model compounds. Upon fitting of the data with MC Kale functions, further evidence is obtained for an unchanged coordination with 4 donor nitrogen ligands when passing from + 0.3 V to + l.15 V. Nevertheless, a considerable change in geometry occurs upon oxydation of the film: at + 0.3 V the geometry around Cu(I) is best described as distorted tetrahedral with 2 Cu-N distances at 2.08 Å and 1.96 Å approximately, while at + l.15 V, the geometry around Cu(II) is flattened tetrahedral with an average Cu-N distance of 2.0l Å Comparison between spectra recorded with freshly-prepared and remetallated via lithium/copper exchange films reveals no evident change in geometry and distances around Cu(I) centers, thus confirming the high reversibility of copper binding. ■

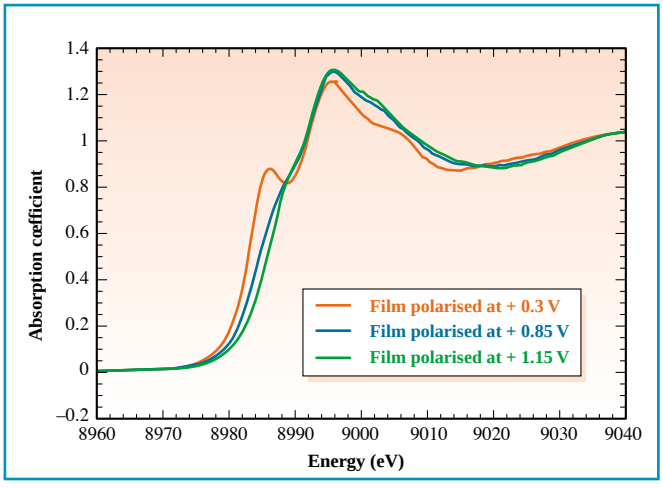

Fig. 3: A shift in the position of the edge shows the oxidation state of the copper centers.

REFERENCE

[l] P.L. Vidal, M. Billon, B. Divisia-Blohorn, G. Bidan, J.M. Kern and J.P. Sauvage, Chem. Commun., 629 (1998).

Modification of the Island Morphology during Metal Epitaxial Growth, due to a Surfactant

J. Alvarez, E. Lundgren, X. Torrelles and S. Ferrer

ESRF, Experiments Division

During the epitaxial growth process of metals or semiconductors, the deposited material forms islands. In order to control this process, it is important to determine parameters such as the dimensions, shapes and densities of the islands. Two-dimensional images show that the island morphology and orientation can be modified by the addition of a surfactant before growth.

Generally speaking, epitaxial growth of metals or semiconductors aims to produce thin films as perfect as possible. This means good crystallinity, low density of defects and surface flatness. In many cases, if the substrate temperature is not too high, the deposited material forms islands at the surface causing significant surface roughness. The dimensions of the islands, their shapes and densities are very important parameters to determine, in order to control the growth process. The morphology of the islands is the result of the competitions of various dynamical processes. Thus, it is important to characterize the morphology during uninterrupted growth, since interruptions could cause further morphological changes.

The diffracted intensity from a rough surface contains information on the short-ranged correlations of the surface. By setting the scattering conditions in an adequate way, one may enhance the diffuse scattering which arises from the surface roughness relative to the long-range order part of the diffracted intensity. We have used a CCD camera to obtain two-dimensional diffuse scattering distributions of the diffracted intensity during uninterrupted epitaxial growth at the Surface Diffraction beamline (ID3).

Atoms of silver were deposited on Ag(100) at a constant rate of about one atomic layer per minute. The diffuse scattering at an early stage of growth when only 0.5 atomic layers were deposited is shown in Figure 1. The image was acquired in 3.7 seconds and it represents a snapshot of a long series of images acquired during the growth process. The diameter of the ring-shaped diffuse intensity provides information on the island sizes and separation. The circular symmetry of the intensity distribution indicates that no azimuthal ordering of the islands takes place at this stage. After further growth, the ring-shaped intensity changes to a four-fold symmetric distribution indicative of relative ordering of the orientation of the islands. Figure 2 shows the result after 27.5 atomic layers have been grown. In this case the image has been taken with a long exposure time (12 minutes) for better clarity of the figure but a snapshot of a few seconds already shows the cross-like intensity distribution of Figure 2. The arms of the cross are along the closest packed lines of substrate atoms. The diffraction pattern is indicative of a pyramidal island morphology.

A manipulation of the morphology of the islands may be done by depositing a small amount (~ 0.1 atomic layer) of a surfactant (Indium in our case), prior to the growth process. The atoms of the surfactant may act as nucleation centres of the islands or enhance surface diffusion, modifying their density. Figure 3 is an image taken after depositing 10.5 atomic layers of Ag on the Ag substrate pre-covered with In. Again, as in Figure 2, the image has been taken with a relatively long exposure time (5 minutes) for clarity. The scales of Figures 2 and 3 are the same. As may be seen, the spread of the diffuse scattering is less in Figure 3 than in Figure 2, indicating that the dimensions of the islands are larger in the case of growth with surfactant. The diffuse intensity shows also a four-fold symmetry indicative of a regularity of the island

Fig. 1: Two-dimensional image of the diffuse scattered intensity during the growth of Ag on Ag(100) at the early stages of the deposition when only 0.5 atomic layers have been deposited. The image was acquired in 3.7 seconds and it represents a snapshot of a series of many images recorded during the growth process. The ring-shaped pattern indicates azimuthal disorder.

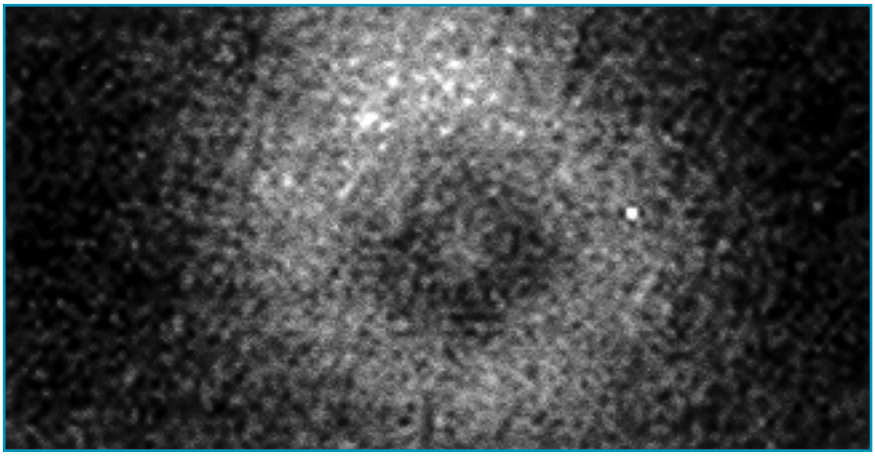

morphology. However, both the shape and the orientation differ markedly from those obtained without surfactant. The symmetry axes of the intensity distribution in Figure 3 are rotated 45 degrees compared to those in Figure 2, indicating that the surfactant has caused the pyramid-like islands to grow in a different orientation. The bases of the pyramids are in this case aligned with the [100] surface directions which consist of lines of atoms separated $\sqrt{2}$ times the nearest neighbor atomic spacing. It appears that in some way the surfactant facilitates surface diffusion along the above directions.

The above examples illustrate how two-dimensional images may reveal very important information that would be inaccessible if only one-dimensional intensity profiles were recorded. ■

Fig. 2: Diffuse scattering distribution after deposition of 27.5 atomic layers. A four-fold symmetry is an evident indicative of ordering.

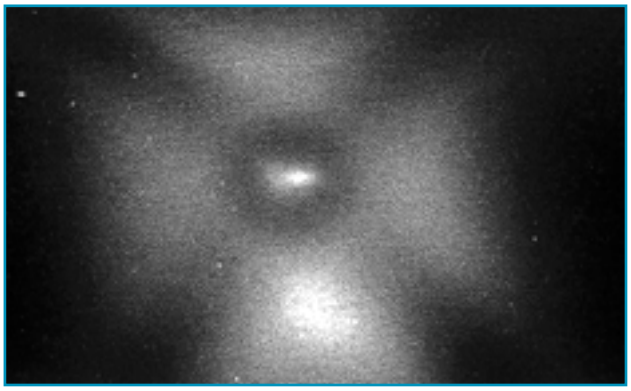

Fig. 3: Diffuse scattering distribution after deposition of 10.5 monolayers of Ag on a Ag(100) surface pre-covered with a small amount of In. The image shows again a four-fold symmetry but the axes are rotated 45° compared to those in Figure 2.

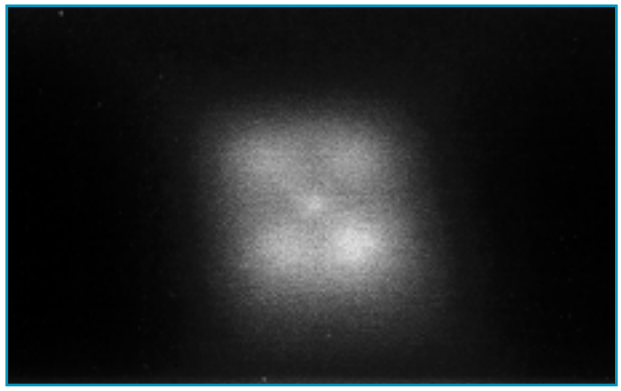

Oxidation of NiAl(100) Studied with Surface Sensitive X-ray Diffraction

A. Stierle[1], V. Formoso[1], F. Comin[1], G. Schmitz[2] and R. Franchy[2]

1 ESRF, Experiments Division
2 IGV-Jülich, Jülich (Germany)

Thin, ordered aluminium oxide layers play a very important role as supports for model catalysts prepared under UHV conditions. Oxidation of NiAl single crystals provides an elegant way to prepare ordered Al_2O_3 layers, which can have different structures depending on the orientation of the NiAl substrate. In addition NiAl is frequently used as a high temperature resistant material. The formation of the protective Al_2O_3 layer is not understood in detail and a microscopic picture of the oxidation process is still missing.

GEED investigations [1] show a (2*1) superstructure after high temperature oxidation and from additional EELS measurements the formation of θ-Al_2O_3 was deduced. The aim of our study was the determination of the Al_2O_3 layer structure and the structure of the Al_2O_3/NiAl(100) interface using surface sensitive x-ray diffraction. The clean sample surface was prepared in the *in situ* UHV surface diffraction chamber of ID32 by several cycles of oxidation and flashing to 1150 °C, which removes the oxide layer and other impurities. Figure 1 shows the structure factor of the clean NiAl(100) surface truncation rods as a function of the reciprocal lattice co-ordinate L normal to the surface.

We tried different models to simulate the data. In model 1 the ideal Ni bulk

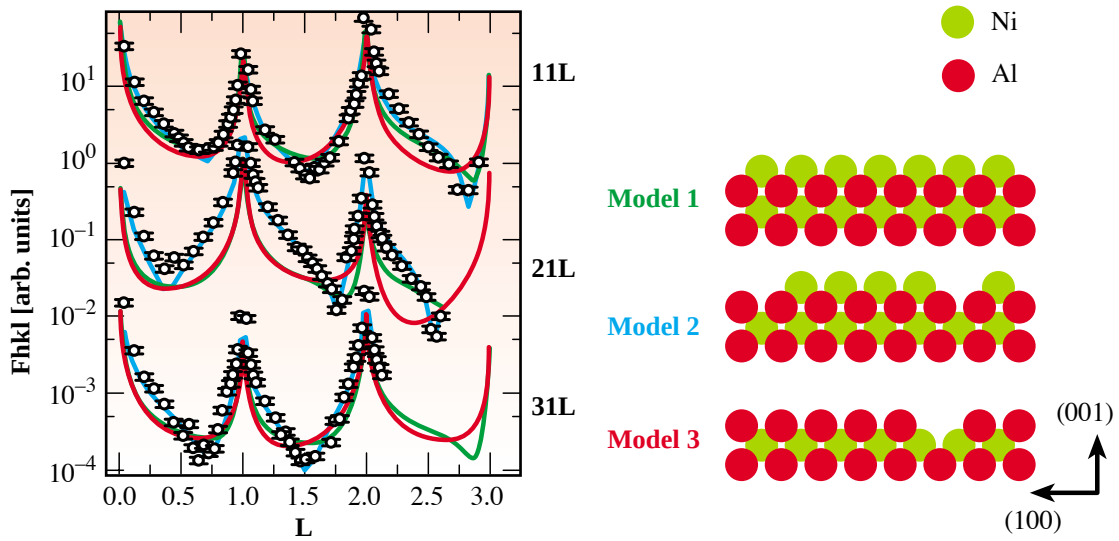

Fig. 1: a) Structure factor F(hkl) as a function of the perpendicular reciprocal lattice co-ordinate L; b) different structural models used to describe the experimental data.

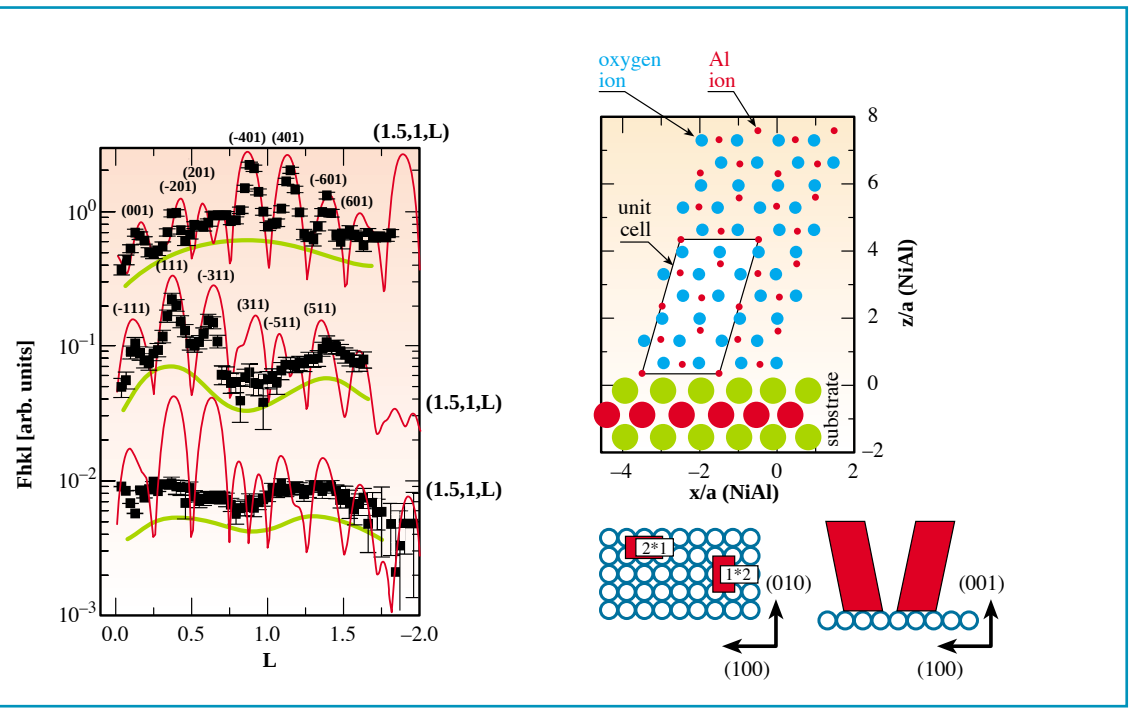

Fig. 2: a) Structure factor F(hkl) of half-order rods after oxidation, b) structural model, c) domain structure.

termination of NiAl with CsCl structure was used and only a relaxation of the first Ni layer was admitted. The simulation could be significantly improved by the introduction of Ni vacancies on the surface (model 2, blue curve) and a 2/3 Ni occupation with 4 % inward relaxation gives the best agreement. An Al terminated surface (model 3), including vacancies and relaxations, is not able to describe the data.

After oxidation at 950 °C for 600 s at $p(O_2)$ = 1 x 10^{-6} mbar half-order rods corresponding to the (2*1) reconstruction appear. In Figure 2 the structure factor as a function of L is plotted for different half-order rods. On all the rods sharper peaks are superimposed on a broad modulation. The red curve is a calculation based on a 2 nm thick monoclinic θ-Al_2O_3 layer; a projection of the structure is shown in Figure 2b. All the peaks observed can be indexed in monoclinic co-ordinates and Figure 2c shows the domain structure of the oxide layer. Besides the (2*1) and (1*2) in-plane domains also twin formation in the growth direction is observed, leading to an inversion of the Al ion layer stacking.

The additional modulation (schematic in green) is attributed to the interfacial structure. At the moment the formation of an Ni_2AlO_4 spinel like interfacial layer is discussed as the origin of the modulation and more detailed model calculations are under its way. ■

Reference

[1] P. Gassmann, R. Franchy, H. Ibach, Surf. Sci. 319, 95 (1994).

Synchrotron Radiation Grazing Incidence X-ray Diffraction: A New Tool for Structural Investigations of Ion-Implanted Glasses

F. D'Acapito and F. Zontone

ESRF, Experiments Division

Composite systems consisting of metallic nanoparticles embedded in glass have recently attracted a great interest in the field of optoelectronics because of their non-linear optical behavior. The implantation process creates a thin (a few hundreds of Å) cluster-rich layer just about 1000 Å below the glass surface. A novel x-ray technique has been developed to carry out structural investigations of such systems. It is based on the signal enhancement from the surface layer with respect to the substrate contribution when working at the critical angle for total external reflection at the implanted layer-substrate interface. By using the refracted beam as a probe, the diffraction profile of the metallic clusters in very diluted samples (a single implant in the 10^{16} at/cm^2 range) can be extracted by a simple subtraction procedure. A demonstration of the new method on SiO_2 glasses implanted with Ag ions is shown in Figure 1. The measurements were performed at the High Pressure station at the ID9 beamline. The samples were illuminated with a 10(h) x 24(v) μm^2 very intense monochromatic beam in the grazing incidence geometry with grazing angles ranging from 0.05 to 0.2°. The data were collected by using an imaging plate system in the q range 0.1 – 8.5 Å^{-1} with integration times in the minute timescale. Curves A and B are the 2θ scattering patterns after integration of the 2D data at the grazing angles for total external reflection at the metal-rich layer-substrate and at the air-substrate interfaces (positions A and B in the reflectivity curve respectively). The profile A shows small diffraction peaks from crystalline phases of the metallic clusters emerging from the smooth amorphous SiO_2 background which disappear in the profile B. After the subtraction procedure ten main peaks are clearly visible in the difference signal coming from the fcc phase of the Ag clusters. The data quality is high enough to enable crystalline phases identification, to retrieve lattice parameters and to determine clusters mean sizes. The results are very useful in complementing information from x-ray spectroscopic (EXAFS) methods and «single particle» investigations with electron techniques (TEM). ■

References

[1] «Characterization of Cu Metallic Clusters in Amorphous SiO_2 by Synchrotron Radiation Grazing Incidence X-ray Scattering and Diffraction» F. D'Acapito, D. Thiaudiere, F. Zontone, J.R. Regnard, Mat. Sci. Forum, Proceedings of the EPDIC-7 Int. Conf., in press.

[2] «Grazing Incidence X-ray Diffraction in the Study of Metallic Clusters Buried in Glass obtained by Ion Implantation» F. D'Acapito, F. Zontone, J. Appl. Cryst. (accepted).

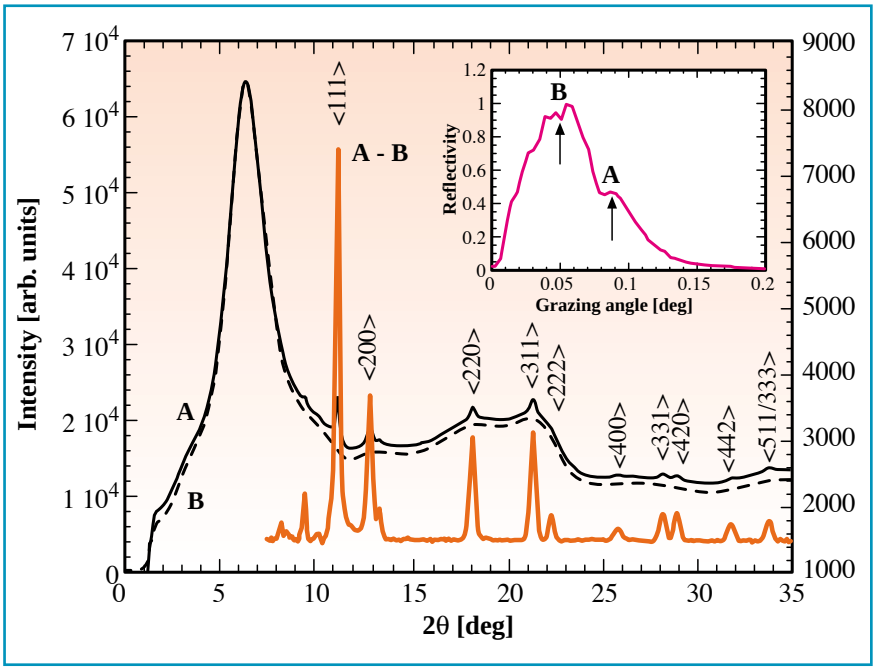

Fig. 1: Extraction of the cluster rich layer signal with the new grazing incidence x-ray method in the case of an Ag implanted SiO_2 glass: the diffraction peaks coming from the cluster are maximized at the total external reflection condition for the glass-clusters layer interface (A case). They are not visible in the profile B. In the difference profile ten main peaks (with indices) are clearly visible related to the fcc phase of the Ag clusters, the other coming from unknown phases. The insert shows the reflectivity curve.

ID27: An Industrial TXRF Facility

F. Comin, M. Navizet, P. Mangiagalli and G. Apostolo
ESRF, Experiments Division

The ESRF-TXRF facility will soon provide silicon manufacturing companies with an analytical centralized TXRF service capable of detection limits for contaminants at the wafer surfaces below 10^8 at/cm^2.

Metallic contaminants at the surface of silicon wafer seriously hinder the performances of integrated circuits. The present non-destructive method used in production plants for measuring surface contamination, Total Reflection X-ray Fluorescence (TXRF) approaches its limits, while the quest for smaller and smaller design rule in device technology imposes lower and lower limits of tolerance. The National Technology Roadmap for Semiconductor published by Sematech, Inc. [1] has already programmed the transition from laboratory-based analytical services to synchrotron-radiation-based installations. In the early 90s the pioneering work of many groups opened the way to the use of synchrotron radiation to industrial TXRF applications [2, 3, 4]. At the ESRF a test experiment was performed a little more than one year ago [5] in order to verify the possibility of attaining the sensitivities envisaged by the Sematech Roadmap while keeping the wafer in a convenient horizontal attitude. The outcome of the test experiment actually showed that the many orders of magnitude of increase in brilliance not only permit the wafer to seat horizontally, but that mapping of the entire wafer surface is also possible in a reasonable amount of time. On the basis of these findings, a project financed by the ESRF, semiconductor companies, research laboratories and the European MEDEA** program was launched in July 1997 for the set-up of an industrial permanent instrument.

The TXRF facility will offer the possibility to map the concentration of contaminants with an initial detection limit of 10^9 at/cm^2 for 1999 to be pushed down to 10^8 at/cm^2 in the following years. The wafer size can be either 200 or 300 mm and the pixel size about one cm^2. The project envisages also the detection of low Z elements at least down to sodium, thus requiring excitation beams below the silicon K threshold.

*** Since 1997, the program «Micro-Electronics Development for European Applications» is meant to assist the European semiconductor industry in developing novel techniques. MEDEA has taken over from JESSI, the «Joint European Submicron Semiconductor Initiative», which ran out in 1996 after 8 years of operation.*

OPTICS

The key issues that have been taken into account for the definition of the optical layout of the installation can be summarized as follows:

- Need of a wide energy range from 1 keV to 40 keV for optimizing the detection sensitivity for every element.
- Need to reject as much as possible the harmonic content of the x-ray beam to limit detection problems with standard solid state energy dispersive detectors.
- Need to preserve the polarization and collimation of the beam for maximum rejection of the elastically scattered radiation at the detector.
- Need of a monochromator with fixed-exit beam to avoid the re-alignment of the wafer position at each change of energy.

THE PHOTON SOURCE

The best way to reject harmonics is, of course, to start without harmonics. The Insertion Devices Group analyzed the possibility of manufacturing an aperiodic undulator that will have the «harmonics» well displaced from where they should be if they were normal harmonics. From their calculation the residual harmonic content of the undulator that is presently under construction is of a few per cent [6]. A further reduction of the harmonic

THE TXRF TECHNIQUE

Total Reflection X-Ray Fluorescence (TXRF) analysis is a powerful tool for the identification and quantification of chemical elements at the fentogram level. TXRF is based on the conventional energy dispersive X-Ray Fluorescence (XRF) analysis technique. The identification of the different elements is obtained by exciting the atoms of the sample with an x-ray beam. Each excited atom will emit a fluorescence photon with a well-defined characteristic energy, which is the signature of its atomic species. The quantitive analysis of the fluorescence spectrum with an energy dispersive detector allows the identification and quantification of the elements present in the sample. TXRF differs from standard XRF only in the particular excitation geometry: the x-ray beam impinges on the sample with a very small glancing angle. Under these conditions the beam penetrates the sample only by a few tens of angströms so that only the shallow region close to the surface is probed. This excitation geometry simultaneously reduces the background and enhances the sensitivity of the technique, which is now perfectly suited for the analysis of surface contamination. The combination of the TXRF technique with synchrotron radiation x-ray beams allows detection limits of the order of 10^8 at/cm^2 for transition metals, which means that a foreign impurity atom can be identified on the wafer surface among ten million silicon atoms.

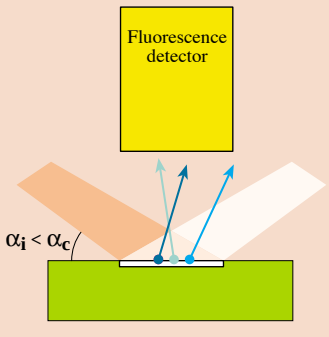

content will be achieved at the monochromator by detuning the Si crystals and by an appropriate choice of multilayers.

THE MONOCHROMATOR

For maximum reliability the x-ray monochromator is based on a single rotation motion following well-established concepts. The dispersing elements are a silicon (111) channel-cut for the energy range 2.8 – 40 keV and a multilayer pair for the low energy range [7]. The high brilliance of the ESRF leaves the possibility of using the sharp Si(111) reflection without deterioration of the TXRF performances. This allows chemical recognition of the impurity atoms by collection of XANES spectra around the threshold of the atomic species of interest.

THE TXRF SET-UP

The TXRF end-station is located in a shielded hutch of about 25 m^2 embedded in a class 100 laminar flow. The station encompasses: a loading robot that transfers the wafers from standard cassettes to a load-lock vessel; a high vacuum handler that transfers the wafer from the interlock loading chamber to the measuring position in the main TXRF chamber, a set of two 7-element linear arrays of Si(Li) detectors for the parallel acquisition of the fluorescence spectra, and a wafer chuck/manipulator for the correct positioning of the wafer onto the x-ray beam and for rotating the wafer around its vertical axis in order to perform the impurity mapping over the whole surface of the wafer.

The 14 channels of the detector are split into two independent arrays for servicing/reliability purposes.

Due to the grazing incidence, the beam illuminates a strip on the sample, the use of 14 independent detector channels, each of which looks to a 10.5 mm wide portion of this strip allows an easy mapping of the entire surface of the wafer just by rotating the sample and collecting data in parallel from the detector array.

This geometry greatly simplifies the mechanical requirements for the wafer handling, but implies that either the spatial resolution or the sensitivity for the outer portion of the wafer is somewhat lower than for the central one.

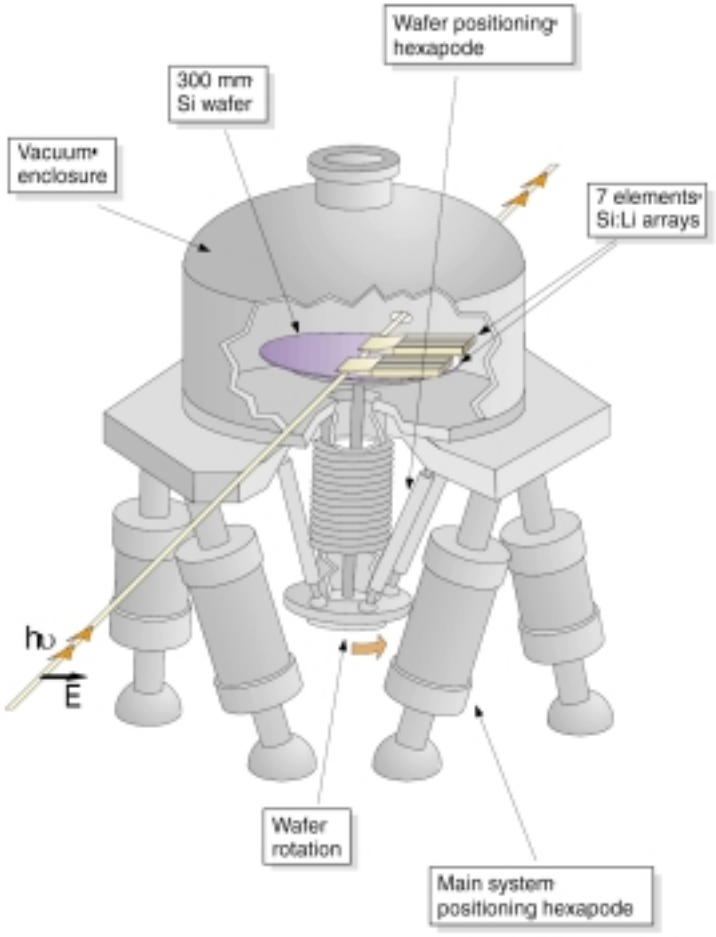

TIME SCHEDULE

The facility will start its commissioning phase early in 1999 with the first tests on real 300 mm wafers. This will lead to a field assessment of the specifications attained and further tests are already envisaged to ascertain which other opportunities can be exploited with the instrument. Two directions seem particularly interesting, namely the possibility of performing XANES spectroscopy in selected atomic species for the chemical identification of the contaminant and the detection of carbon species via electron spectroscopy techniques. ■

REFERENCES

[1] http://notes.sematech.org/97melec.html.

[2] A. Iida, Adv. In X-ray Anal., 35 (1992) 795.

[3] R. Rieder et al., Nucl. Instr. and Meth. In Phys. Res. A355, 648-653 (1995).

[4] P. Pianetta et al. Rev. Sci. Instrum. 66, 1293 (1995).

[5] L. Ortega et al., Journal of Synch. Radiation, 5, 1064-1066 (1998).

[6] J. Chavanne et al., EPAC 98 conference, Stockholm.

[7] F. Comin et al., SPIE Proc. Intern. Symp. On Optical Science, Eng., and Instr. San Diego, July (1998).

A Third Acceleration Unit for the ESRF Storage Ring

C. David, J. Jacob, A. Panzarella, J.P. Perrine and J.L. Revol

ESRF, Machine Division

After only two years of design, construction and commissioning, a new acceleration unit is now in operation on the ESRF storage ring. It allows all klystrons and cavities to be run at moderate power even for high intensity operation at 200 mA, whilst still gaining in total accelerating voltage, from 8 to 12 MV. The third pair of cavities can also be used to modulate the radio-frequency voltage at the revolution frequency, thereby producing additional damping of longitudinal multibunch oscillations. The planning and commissioning constraints imposed by the installation of this equipment on a running machine was one of the challenging issues. The project was managed so as to minimize the inconvenience for ESRF users.

Four 352.2 MHz five-cell cavities and two 1.0 MW Radio Frequency (RF) transmitters (upgraded to 1.3 MW in January 94) were initially installed on the ESRF storage ring for an operation at the design current of 100 mA at 6 GeV. During the commissioning of the storage ring, it was already possible to store higher currents and 200 mA of beam current have been delivered to the users in multibunch operation since November 1995. This resulted in pushing the power through the cavity input couplers to very high values and required operating the storage ring with both RF transmitters, each feeding one pair of cavities with up to 750 kW.

In early 1995 it was decided to construct a third RF transmitter (SRRF3) feeding a third pair of cavities [1]. Besides the reduced power load for the cavity couplers and a gain in redundancy, this third RF unit opens up other interesting new features.

DESIGN AND CONSTRUCTION

Based on experience gained from the existing RF units, it was decided to construct the third RF unit using similar hardware for the large components. This includes the klystrons, the high voltage power supply, the circulator, parts of the low level RF and the five-cell cavities [1, 2, 3, 4].

The 100 kV - 22 A DC power supply for the third klystron was ordered in September 95 from the constructor and mounted and cabled under our responsibility: it was a very successful approach both in terms of cost savings and transfer of expertise to the RF crew. It also eased the implementation of an improved local control and of special measures against interference with the remaining RF equipment. The high-voltage power supply was ready as scheduled at the end of February 97.

A new control system was developed for SRRF3 and commissioned in parallel with the hardware [5]:

- The object-oriented programming approach based on the separation between the transmitter and the cavities, which are themselves split into basic devices, proved to be very versatile for the development.
- The hardware protection is managed independently from the control software by a PLC for the slow interlocks and a hardwired system for the fast protections.
- The diagnostics tools included in the design are very useful for trip analysis and parameter follow up.
- The operator controls the RF system via an easy-to-use graphical user interface.

Some sensitive parts of the RF system, such as the arc detection system, have been redesigned in order to reduce the rate of spurious triggering. Also the cavity vacuum equipment has been improved:

- The fast pressure interlock system, which is essential for the ceramics protection against glow discharges with subsequent sputter deposition of copper [3], has been doubled (two fast pressure detectors per cavity).
- The NEG pumps of the old design have been replaced by titanium sublimation pumps. This proved to be very efficient during RF conditioning and commissioning with beam, as it was possible to activate these pumps regularly, so that the vacuum could recuperate quickly after a strong outgassing.

COMMISSIONING AND OPERATION

The new SRRF3 transmitter was ready for commissioning with beam on the scheduled date in August 97. After only four days, 160 mA could be stored and were then delivered for the first week of user service mode. The maximum ESRF current of 205 mA was reached one week later and served routinely in the 4th week of User Service Mode.

The failure rate was higher during the commissioning period and the beam availability was reduced (90% instead of the usual 95%). After only three months of operation, the mean time between failures was recovered and is steadily increasing.

During the three first months of operation, a lot of trips were caused by bursts of reflected power from the cavities, which were typically 50 μs long and as high as 300 kW at the peak. These events were mostly associated with outgassing and were probably due to fast detuning provoked by multipactor in one of the five cells. Continuous operation of the cavities was the only cure for these trips which steadily became less and less frequent.

In the early stage of commissioning, we were also confronted with high harmonic power generated by the

klystron. The harmonics are fed back to the klystron by the reflection from the circulator, which is only matched at the fundamental RF frequency. Careful adjustment and positioning of matching elements (iris, post) allowed the harmonic power to be brought to an acceptable level.
A part of the early failures were removed gradually during the first three months simply by debugging the system. The high voltage power supply proved to be very reliable.

NEW POSSIBILITIES

More flexibility and larger safety margin

The fact that the maximum ESRF beam current of 205 mA can be stored without SRRF2 represents a large gain in flexibility and security. Klystron acceptance tests, cavity coupler conditioning and extensive R&D work requiring RF power can now be performed without restriction for the ESRF users.
It is planned to extend the waveguide network such that SRRF2 can replace either SRRF1 or even the booster RF system. By doing this, we will obtain a level of redundancy that will allow the operation of the storage ring to be safeguarded even in case of a major failure on any single transmitter.

Increase in cavity voltage

The third pair of cavities has allowed the cavity voltage to be raised from 8 to 12 MV with only a negligible increase in total power and still a reduction of the power per cavity coupler. However, it turned out that the associated gain in longitudinal acceptance did not show up on the lifetime which is presently limited by the transverse acceptance. Increasing the transverse acceptance of the storage ring is therefore one topic of machine physics studies to fully benefit from the enlarged longitudinal acceptance.
Since in single-bunch and 32-bunch operation the lifetime is also Touschek limited, the optimum voltage was found to be close to 8 MV, for which the bunches are longest and the energy acceptance is not yet limited by the RF.

Landau damping** of multibunch instabilities with cavities 5 & 6

For standard high intensity operation, only 2/3 of the storage ring is filled to produce strong transient beam loading, which leads to a voltage modulation at the revolution frequency f_0. The subsequent spread in synchrotron frequencies provides Landau damping of longitudinal multibunch instabilities which are driven by Higher Order Modes (HOM) developing in the cavities, a point of major importance for the ESRF [6]. An additional feature of the third RF system is the possibility to operate it at $f_{RF} + f_0$, such as to modulate the total RF voltage actively even for symmetrical fillings [7].
The detuned fundamental modes of cavities 5 & 6 can be used intentionally to launch an n = 1 multibunch instability. The threshold current is increased by a factor 4 when applying a modulation voltage of 1.5 MV. This scheme is employed for operation with 32 equally-spaced bunches in the storage ring. In this operation mode the optimum voltage of about 8 MV requires switching off cavities 5 & 6. As these are no longer temperature regulated, modulation is necessary to operate untroubled by multibunch instabilities at the nominal intensity of 90 mA.

Basis for an upgrade of the existing transmitters

After the successful commissioning of SRRF3, the new control system is now fully validated. From the high UNIX level down to the hardwired fast interlock system, it had been designed taking into account the necessity of upgrading the existing RF units. Thanks to the existence of SRRF3, this work is now possible in parallel to operating the storage ring at full intensity.
Based on the clear separation between cavity and transmitter control, we are able to proceed in two steps. We will first transfer the cavities 1 to 4 from the initial to the new control system. This will take place in the next October shutdown. The upgrade of the transmitters will then take place one by one.

CONCLUSION

The third RF acceleration unit was successfully built and put into operation. It was fully designed by ESRF staff in order to best match the operation constraints and specificities, and to fit into the ESRF environment, taking into account the experience gained on the existing RF units. Performing such a design and construction work was very beneficial for broadening the knowledge and expertise of our RF group personnel. The project was completed within its budget and on schedule, and was managed so as to minimize the inconvenience for ESRF users. This was a challenging issue for a machine which delivers 5600 hours of x-ray beam per year. ■

ACKNOWLEDGEMENTS

The authors wish to thank the numerous colleagues from the Technical Services, the Computing Services, the Safety Group and the Machine Division for their contribution to the success of the SRRF3 project, and particularly: P. Barbier, D. Boilot, B. Boucif, M. De Donno, H. Delamare, M. Dubrulle, G. Gautier, P. Kernel, J.M. Mercier, J. Meyer, N. Michel, O. Naumann, J.L. Pons, E. Rabeuf, D. Vial.

REFERENCES

[1] J. Jacob et al., «Construction of a Third RF Acceleration Unit for the ESRF Storage Ring», EPAC'96, Barcelona, June 1996.
[2] J. Jacob et al., «Commissioning and Operation of one Booster and two Storage Ring RF Acceleration Units at the ESRF», EPAC'92, Berlin, March 1992.
[3] J. Jacob et al., «RF System Development for High Current Accumulation in the ESRF Storage Ring», EPAC'94, London, June 1994.
[4] J. Jacob et al., «Commissioning of the Third RF Acceleration Unit for the ESRF Storage Ring», EPAC'98, Stockholm, June 1998.
[5] J.-L. Revol et al., «An Object Oriented Control System for the Third Storage Ring RF Unit at the ESRF», EPAC'98, Stockholm, June 1998.
[6] O. Naumann and J Jacob, «Fractional Filling Induced Landau Damping of Longitudinal Instabilities at the ESRF», PAC'97, Vancouver, May 1997.
[7] O. Naumann and J. Jacob, «Landau Damping of Longitudinal Instabilities for the Operation of the ESRF Storage Ring», EPAC'98, Stockholm, June 1998.

** The Landau damping decreases the energy spread of the beam induced by coupled bunch oscillations and increases the bunch length (which also means the Touschek lifetime).

Events

HERCULES 1998

(See article on page 4)

Next HERCULES Course

21 February - 1 April 1999

Deadline for application: 16 October 1998 • e-mail: simpson@polycnrs-gre.fr

Next USERS' MEETING

11-12 February 1999

(See article on page 5)

The ESRF Newsletter is published by the European Synchrotron Radiation Facility
BP 220, F38043 Grenoble cedex
Editor: Dominique CORNUÉJOLS Tél (33) 4 76 88 20 25

Dépôt légal : 3eme trimestre 1998. Printed in France by Repro-Express. Layout by Pixel Project.